Ananda Bandara, 1

1   **The necrotrophic fungus *Macrophomina phaseolina* induces oxidative stress-associated genes**

2   **and related biochemical responses in charcoal rot susceptible sorghum genotypes**

3

4   Ananda Y. Bandara., Dilooshi K. Weerasooriya., Sanzhen Liu., and Christopher R. Little*

5

6

7   Ananda Y. Bandara (anandayb@ksu.edu), Sanzhen Liu (liu3zhen@ksu.edu) and Christopher R.

8   Little (crlittle@ksu.edu): Department of Plant Pathology, Kansas State University, Manhattan, KS,

9   66506, USA., Dilooshi K Weerasooriya (dilooshi@ksu.edu): Department of Agronomy, Kansas

10   State University, Manhattan, KS, 66506, USA

11

12

13

14   *Corresponding author: Christopher R Little

15

16

17 **ABSTRACT**

18

19 *Macrophomina phaseolina* (MP) is a necrotrophic fungus that causes charcoal rot disease in

20 sorghum [*Sorghum bicolor* (L.) Moench]. The host resistance and susceptibility mechanisms for

21 this disease are poorly understood. Here, the transcriptional and biochemical aspects of the

22 oxidative stress and antioxidant system of charcoal rot resistant and susceptible sorghum

23 genotypes in response to MP inoculation were investigated. RNA sequencing revealed 96

24 differentially expressed genes between resistant (SC599) and susceptible (Tx7000) genotypes that

25 are related to the host oxidative stress and antioxidant system. Follow-up functional experiments

26 demonstrated MP's ability to significantly increase reactive oxygen (ROS) and nitrogen species

27 (RNS) content in the susceptible genotypes. This was confirmed by increased malondialdehyde

28 content, an indicator of ROS/RNS-mediated lipid peroxidation. The presence of nitric oxide (NO)

29 in stalk tissues of susceptible genotypes was confirmed using a NO-specific fluorescent probe

30 (DAF-FM DA) and visualized by confocal microscopy. Inoculation significantly increased

31 peroxidase activity in susceptible genotypes while catalase activity was significantly higher in MP-

32 inoculated resistant genotypes. MP inoculation significantly reduced superoxide dismutase activity

33 in all genotypes. These findings suggested MP's ability to promote a host-derived oxidative stress

34 response in susceptible sorghum genotypes, which contributes to induced cell death-associated

35 disease susceptibility to this necrotrophic phytopathogen.

36

37

38

39

40   **INTRODUCTION**

41

42   Plants defend themselves from pathogens using numerous defense mechanisms. Pathogen-

43   associated molecular patterns (PAMPs) are elicited by plants as a less specific recognition system

44   to prevent pathogen invasion, to restrict pathogen growth, and contribute to basal defense (Jones

45   and Dangl 2006). Plants produce resistance proteins in response to pathogen infections that

46   overcome basal defense. These proteins promote inducible defense responses often characterized

47   by a hypersensitive response (HR)-associated host cell death upon pathogen recognition. HR

48   constrains the invasion of biotrophic pathogens and subsequent pathogen growth as biotrophs

49   derive their energy requirements from living host cells. Necrotrophic pathogens, on the other hand,

50   actively kill host tissue as they colonize and obtain nutrients from dead or dying cells (Stone 2001).

51   Therefore, any mechanism that results in host cell death including HR is beneficial for necrotroph

52   pathogenesis. Cell death during HR is dependent upon the balanced production of nitric oxide

53   (NO) and reactive oxygen species (ROS) (Delledonne et al. 2001). Many necrotrophs produce

54   ROS as virulence factors during colonization (Shetty et al. 2008). For example, the infection,

55   colonization, and suppression of host defenses by the model necrotrophic fungus, *Botrytis cinerea*

56   is due to the production of high levels of ROS (van Kan 2006; Choquer et al. 2007). *Macrophomina*

57   *phaseolina* generates a flux of NO during the infection process of jute plant (Sarkar et al. 2014).

58

59   *M. phaseolina* has been reported to cause root and stalk rot in > 500 plant species (Islam et al.

60   2012), including food crops (Su et al. 2001), pulse crops (Mayek-Pérez et al. 2001; Raguchander

61   et al. 1993), fiber crops [jute (De et al. 1992), cotton (Aly et al. 2007)], and oil crops (Wyllie 1998).

62   *M. phaseolina* causes charcoal rot disease in many economically important crops including

63   sorghum, soybean, maize, alfalfa and jute (Islam et al. 2012). This soilborne, necrotrophic fungus

64   occurs across a wide geographic region including tropical and temperate environments (Tarr 1962;

65   Tesso et al. 2012). Charcoal rot in sorghum is characterized by degradation of pith tissue at or near

66   the base of the stalk causing the death of stalk pith cells (Edmunds 1964). In this disease, root and

67   stalk cortical and vascular tissues become damaged, which reduces water translocation and nutrient

68   absorption (Hundekar and Anahosur 2012).

69

70   Sorghum is a staple cereal crop for many people in the marginal, semi-arid environments of Africa

71   and South Asia. The unique capability of sorghum to grow in low and variable rainfall regions

72   reveals its suitability to enhance agricultural productivity in water-limited environments (Rosenow

73   et al. 1983). Around the world, sorghum is used as a source of food, feed, sugar, and fiber. With

74   the recent interest in bioenergy feedstocks, sorghum has been recognized as a promising alternative

75   for sustainable biofuel production (Kimber et al. 2013). Recent studies have revealed the negative

76   impacts of charcoal rot disease on grain sorghum physicochemical properties (Bandara et al.

77   2017a), yield components (Bandara et al. 2017b), and the staygreen trait (Bandara et al. 2016), as

78   well as the biofuel traits of sweet sorghum (Bandara et al. 2018a; Bandara et al. 2017c). As

79   charcoal rot is a high priority fungal disease in sorghum [*Sorghum bicolor* (L.) Moench], that

80   causes crop losses where ever sorghum is grown (Tesso et al. 2012), more research is needed to

81   identify charcoal rot resistance/susceptibility mechanisms. A recent study showed that *M.*

82   *phaseolina* promotes charcoal rot susceptibility in grain sorghum via induced host cell-wall-

83   degrading enzymes such as cellulase, pectin methylesterase, and polygalacturonase (Bandara et al.

84   2018b).

85

86

87   Although some necrotrophic fungi use their own ROS and reactive nitrogen species (RNS) as

88   virulence factors during infection and colonization (Shetty et al. 2008; van Kan 2006; Choquer et

89   al. 2007; Sarkar et al. 2014), necrotroph infection-associated up-regulation of host-derived ROS

90   and RNS is poorly described. To investigate the differentially expressed genes associated with

91   host-derived oxidative stress, the global transcriptome profiles of charcoal rot resistant (SC599)

92   and susceptible (Tx7000) sorghum lines were characterized in response to *M. phaseolina*

93   inoculation using RNA-Seq. Moreover, follow up functional and biochemical studies in relation

94   to oxidative stress, nitric oxide biosynthetic capacity, the level of lipid peroxidation, and the

95   antioxidant system of charcoal resistant (SC599, SC35) and susceptible (Tx7000, BTx3042)

96   sorghum genotypes after inoculation are reported.

97

98

99   **RESULTS**

100

101   **Differential gene expression analysis**

102

103   The DESeq2 analysis conducted to identify genes with significant genotype $\times$ treatment interaction

104   (see 'Materials and Methods') revealed 2317, 7133, and 432 differentially expressed genes (DEG)

105   at 2, 7, and 30 DPI, respectively. However, only 588, 1718, and 100 of them had assigned

106   metabolic pathways (SorghumCyc database). The 588 and 1718 DEG were constituents of 14 and

107   106 significantly enriched metabolic pathways while no significantly enriched pathway was

108   observed at 30 DPI. Pathway enrichment analysis revealed the greatest expression profile

109   differences between resistant and susceptible genotypes at 7 DPI in response to pathogen infection

110   as the highest number of enriched pathways occurred at that time. Therefore, for interpretation

111   purposes, this paper focuses on the transcriptional data at 7 DPI. At 7 DPI, 96 oxidative stress and

112   antioxidant system-related genes were found to be differentially expressed between charcoal rot

113   resistant and susceptible genotypes in response to *M. phaseolina* inoculation (Figure 1;

114   Supplementary Table 1) and are described below.

115

116   **Differentially expressed genes involved in host ROS biosynthesis**

117

118   In the endoplasmic reticulum, NAD(P)H-dependent electron transport involving cytochrome P450

119   (CP450) produces superoxide anions ($O_2{}^{\bullet-}$) (Mittler 2002). Moreover, the up-regulation of CP450

120   results in increased conversion of endogenous compounds into reactive metabolites and is a source

121   of oxidative stress (Nebert et al. 2000). Therefore, increased CP450 expression is a direct

122   indication of the enhanced oxidative stress. In the current study, a number of cytochrome P480

123   genes involved in acetone degradation (to methylglyoxal), betanidin degradation, brassinosteroid

124   biosynthesis II, free phenylpropanoid acid biosynthesis, gibberellic acid biosynthesis, jasmonic

125   acid biosynthesis, lactucaxanthin biosynthesis, nicotine degradation II, nicotine degradation III,

126   phaseic acid biosynthesis, and phenylpropanoid biosynthesis were differentially expressed

127   (Supplementary Table 1). Moreover, 38 differentially expressed CP450 genes did not have

128   assigned metabolic pathways (Supplementary Table 1). Out of these 38, fourteen were

129   significantly down-regulated in the susceptible genotype while 22 were significantly up-regulated

130   (Figure 1), which contributed to a +42.1 log2-fold net up-regulation of CP450 genes in the

131   susceptible genotype (Supplementary Table 1).

132

133 NADPH oxidases catalyze the synthesis of $O_2^{\bullet-}$ in the apoplast (Sagi and Fluhr 2006). A gene that

134 encodes an NADPH oxidase (*Sb0621s002010*) was significantly down-regulated (log2-fold = –

135 3.2) in Tx7000 after *M. phaseolina* inoculation (Supplementary Table 1) while the gene in SC599

136 was not significantly differentially expressed.

137

138 Copper amine oxidases and flavin-containing amine oxidases contribute to defense responses

139 occurring in the apoplast through H_2O_2 production following pathogen invasion (Cona et al. 2006,

140 Wimalasekera et al. 2011). In the current study, four genes that encode for flavin-containing amine

141 oxidases were differentially expressed (Supplementary Table 1), and two of them were

142 significantly up-regulated in pathogen-inoculated Tx7000 (*Sb06g032450*, *Sb06g032460*; log2-fold

143 = +0.92, +4.10, respectively), while the other two were significantly down-regulated

144 (*Sb01g044230*, *Sb07g005780*; log2-fold = –4.96, –2.04, respectively). Another gene that encodes

145 for an amine oxidase-related protein (*Sb01g006160*) was significantly down-regulated (log2-fold

146 = –1.39) in Tx7000. Two of the three genes that encoded for a copper methylamine oxidase

147 precursor (*Sb04g028410*, *Sb02g036990*) were significantly down-regulated in pathogen-

148 inoculated Tx7000 (log2-fold = –3.71, –2.84, respectively) while the other (*Sb06g020020*) was

149 significantly up-regulated (log2-fold = +3.33).

150

151 NADH dehydrogenase is a major source of ROS production in mitochondria (Moller 2001; Arora

152 et al. 2002). Oxygen is reduced into $O_2^{\bullet-}$ in the flavoprotein region of NADH dehydrogenase

153 segment of the respiratory chain complex I (Arora et al. 2002). In the current study, two genes that

154 encodes for the NADH dehydrogenase 1 alpha sub-complex, assembly factor 1 (*Sb03g033415*,

155   log2-fold = +2.14) and a NADH dehydrogenase iron-sulfur protein 4 (*Sb02g037780*, log2-fold =

156   +0.97) were significantly up-regulated in pathogen-inoculated Tx7000 (Supplementary Table 1).

157

158   **Differentially expressed genes involved in host NO biosynthesis**

159

160   NO plays a key role in plant immune responses such as the hypersensitive response (HR) during

161   incompatible plant-pathogen interactions (Delledonne et al. 1998; Durner et al. 1998; Yoshioka et

162   al. 2011). The nitrate reduction I and citrulline-nitric oxide cycles are the primary NO biosynthetic

163   pathways in plants (Planchet and Kaiser 2006). In the current study, six genes (*Sb01g039180*,

164   *Sb04g000530*, *Sb05g000240*, *Sb07g024150*, *Sb09g002030*, and *Sb10g002510*) involved in the

165   citrulline-nitric oxide cycle that encode for six isozymes of nitric oxide synthase (EC 1.14.13.39)

166   were significantly down-regulated in Tx7000 after *M. phaseolina* inoculation (Figure 1;

167   Supplementary Table 1). Compared to mock-inoculated control, this was a –12.1 net log2-fold

168   down-regulation. Interestingly, five genes (*Sb03g039960*, *Sb04g025630*, *Sb04g027860*,

169   *Sb05g000680*, and *Sb08g011530*) involved in the nitrate reduction I pathway were significantly

170   up-regulated in pathogen-inoculated Tx7000 and encoded for isozymes of nitrite reductase (NO-

171   forming) (EC 1.7.2.1), marking a +26.8 net log2-fold up-regulation compared to the control

172   treatment. Moreover, three genes (*Sb04g007060*, *Sb07g022750*, and *Sb07g026290*) involved in

173   the nitrate reduction II (assimilatory) pathway that encode for NADH-cytochrome b5 reductase

174   (EC 1.7.1.1) were significantly down-regulated (net log2-fold = –7.61) in pathogen-inoculated

175   Tx7000.

176

177   **Differentially expressed genes involved in the antioxidant system**

178

179   Thirty genes with peroxidase activity (Figure 1; Supplementary Table 1) were differentially

180   expressed between SC599 and Tx7000 after *M. phaseolina* inoculation. Eleven of these genes were

181   significantly down-regulated in Tx7000 while 14 were significantly up-regulated, resulting in a

182   +13.3 net log 2-fold up-regulation. A gene that encodes for catalase (*Sb01g048280*) was

183   significantly down-regulated (log 2-fold = –3.23) in Tx7000 while a superoxide dismutase gene

184   (*Sb07g023950*) was differentially expressed between genotypes after pathogen infection.

185

186   **Analysis of variance (ANOVA) for functional assays**

187

188   The two-way interaction between genotype and inoculation treatment was significant for

189   ROS/RNS, peroxidase, catalase, and TBARS assays at all three post-inoculation stages (4, 7, and

190   10 DPI) (Table 1). SOD activity was an exception where genotype had a significant main effect at

191   4 DPI while both genotype and inoculation treatment had significant main effects at 7 and 10 DPI.

192

193   *M. phaseolina* **inoculation induces ROS and RNS accumulation in charcoal rot susceptible**

194   **genotypes**

195

196   To investigate the potential differences of oxidative stress imposed by *M. phaseolina* on charcoal

197   rot resistant and susceptible sorghum genotypes, the total free radical population (representative

198   of both ROS and RNS) in mock- (control) and pathogen-inoculated samples were measured at

199   three post-inoculation stages. Compared to control, *M. phaseolina* significantly increased the ROS

200   and RNS content of both susceptible genotypes (BTx3042 and Tx7000) at all three post-

201   inoculation stages (4, 7, and 10 DPI) (Figure 2). The percent increase for BTx3042 compared to

202   control was +70.5, +52.5, and +123.8 at 4, 7, and 10 DPI, respectively, while the same for Tx7000

203   was +185.1, +47.3, and +81.9. *M. phaseolina* inoculation did not significantly affect the ROS and

204   RNS content of the two resistant genotypes, SC599 and SC35. Although not statistically

205   significant, ROS and RNS content of *M. phaseolina*-inoculated SC599 was lower than the control

206   at 10 DPI. The same phenomenon was observed for SC35 at 4 and 7 DPI.

207

208   ***M. phaseolina* inoculation induces NO accumulation in charcoal rot susceptible genotypes**

209

210   The bright green fluorescence observed in the infected stalk cross-sections of Tx7000 and

211   BTx3042 at 7 DPI indicated NO-specific fluorescence when stained with DAF-FM DA (Figure

212   3). This revealed the ability of *M. phaseolina* to induce NO biosynthesis and accumulation in

213   charcoal rot susceptible sorghum genotypes. NO-specific fluorescence was absent in control tissue

214   sections (Figure 3), which indicated that induction of NO occurred only after inoculation with the

215   pathogen. Neither mock- nor pathogen-inoculation produced NO-specific fluorescence in the

216   resistant genotypes, SC599 and SC35 (Figure 3). Therefore, the resistant genotypes tested in this

217   study did not undergo NO burst-mediated oxidative stress after *M. phaseolina* infection.

218

219   **Impact of *M. phaseolina* inoculation on sorghum antioxidant enzymes**

220

221   Peroxidases (PX) and catalases (CAT) are important antioxidant enzymes involved in

222   decomposing hydrogen peroxide into water (Hammond-Kosack and Jones 1996). *M. phaseolina*

223   inoculation significantly increased PX activity (mU/mL) in both susceptible genotypes at all post-

224   inoculation stages (Figure 4). The percent activity increase for BTx3042 was +36.9, +41.6, and

225   +37.6% at 4, 7, and 10 DPI, respectively, while the same for Tx7000 were +89.0, +37.0, and

226   +25.9%. *M. phaseolina* inoculation did not significantly affect the PX activity of the two resistant

227   genotypes, SC599 and SC35. Although not significant, SC599 and SC35 had reduced PX activity

228   in comparison to their respective controls at three post-inoculation stages.

229

230   Compared to their respective controls, the CAT activity (U/mL) of the two resistant genotypes was

231   significantly increased after *M. phaseolina* inoculation at all three post-inoculation stages (Figure

232   5). The percent activity increase for SC599 was 50.8, 33.8, and 29.5% at 4, 7, and 10 DPI,

233   respectively, while the same for SC35 was +104.4, +55.5, and +97.8. SC599 exhibited a general

234   trend of declining activity over time with both control and pathogen inoculations. SC35 followed

235   increased and decreased activity over time for both treatments. Interestingly, *M. phaseolina*

236   inoculation significantly decreased the CAT activity of BTx3042 (–38.1%) and Tx7000 (–39.3%)

237   at 7 DPI, although no significant impact was observed at 4 and 10 DPI.

238

239   Superoxide dismutase (SOD) is an antioxidant enzyme responsible for regulating superoxide

240   anions. It converts superoxide to hydrogen peroxide, which can be subsequently detoxified into

241   water through peroxidase and catalase activity (Hammond-Kosack and Jones 1996). In this study,

242   SOD activity was not sorghum genotype-specific. Although *M. phaseolina* inoculation did not

243   significantly affect SOD activity at 4 DPI, it significantly decreased activity at 7 and 10 DPI across

244   the four genotypes (Figure 6). SOD activity was reduced by –14.7 and –15.6% at 7 and 10 DPI,

245   respectively. SOD activity of the four genotypes was not significantly different from each other at

246   4 DPI across inoculation treatments (Figure 6). However, SOD activity in SC35 decreased over

247   time and became significantly lower than BTx3042 and Tx7000 at 7 DPI. At 10 DPI, SC35

248   exhibited significantly less activity than the other genotypes.

249

250   *M. phaseolina* **inoculation enhances lipid peroxidation in charcoal rot susceptible genotypes**

251

252   The degree of lipid peroxidation, as indicated by malondialdehyde (MDA) content is a direct

253   indicator of the degree of oxidative stress experienced by plants (Sharma et al. 2012). *M.*

254   *phaseolina* inoculation significantly increased MDA content (μM) in both charcoal rot susceptible

255   genotypes at all three post-inoculation stages (Figure 7). Compared to control, the increase in

256   MDA after inoculation in BTx3042 was +124.0, +54.4, and +80.6% at 4, 7, and 10 DPI,

257   respectively, while the same for Tx7000 was +262.4, +70.0, and +75.0%. *M. phaseolina*

258   inoculation did not significantly affect MDA content in the two resistant genotypes, SC599 and

259   SC35. In general, SC35 showed higher MDA content at 4 and 7 DPI for both control and pathogen

260   inoculations compared to the other genotypes (Figure 7). However, there was a dramatic MDA

261   drop from 7 to 10 DPI with both control and pathogen inoculations for SC35.

262

263

264   **DISCUSSION**

265

266   *M. phaseolina* **infection induces host oxidative stress and contribute to induced charcoal rot**

267   **susceptibility**

268

269 The synthesis and accumulation of ROS in plants as a defense response to pathogen attack have

270 been well described (Dangl and Jones 2001; Torres et al. 2002). Apoplastic synthesis of superoxide

271 ($O_2^{\bullet-}$) and its dismutation product hydrogen peroxide (H_2O_2) has been reported in response to a

272 variety of pathogens (Doke 1983; Auh and Murphy 1995; Grant et al. 2000). Although ROS

273 accumulation typically correlates with active disease resistance reactions against biotrophic or

274 hemibiotrophic pathogens (Vanacker et al. 2000; Allan and Fluhr 1997), certain necrotrophs

275 induce ROS synthesis in the infected tissue to promote cell death that facilitates subsequent

276 infection (Govrin and Levine 2000; Foley et al. 2016). In fact, ROS-mediated defense responses,

277 effective against biotrophic pathogens, increase the susceptibility to necrotrophic pathogens

278 (Kliebenstein and Rowe 2008). The current study provided transcriptional and functional evidence

279 for the ability of necrotrophic fungus *M. phaseolina* to induce ROS and RNS in charcoal rot

280 susceptible sorghum genotypes (Tx7000, BTx3042).

281

282 In the endoplasmic reticulum, the CP450 involved in the NAD(P)H-dependent electron transport

283 chain contributes to $O_2^{\bullet-}$ production (Mittler 2002). In this study, a net up-regulation of CP450s

284 was observed in the susceptible genotype Tx7000, which potentiates NAD(P)H-dependent $O_2^{\bullet-}$

285 production in the endoplasmic reticulum. Therefore, the endoplasmic reticulum appears to be a

286 ROS-generating powerhouse, contributing to enhanced oxidative stress in Tx7000 after *M.*

287 *phaseolina* inoculation. In the apoplast, NADPH oxidases catalyze the synthesis of $O_2^{\bullet-}$ (Sagi and

288 Fluhr 2006). NADPH oxidases are also involved in ROS production in response to pathogen

289 infections (Sagi and Fluhr 2001; Torres et al. 2002). Fungal NADPH oxidases have been shown

290 to be required for the pathogenesis of certain necrotrophic fungi such as *Sclerotinia sclerotiorum*

291 (Kim et al. 2011), *Botrytis cinerea* (Segmueller et al. 2008), and *Alternaria alternata* (Yang and

292   Chung 2012). In the current study, the observed down-regulation of a host NADPH oxidase gene

293   (*Sb0621s002010*) suggested that apoplastic $O_2^{\bullet-}$ is not a significant source of *M. phaseolina*-

294   induced oxidative stress in Tx7000.

295

296   Amine oxidases are involved in apoplastic H_2O_2 production (Cona et al. 2006, Wimalasekera et

297   al. 2011). Genes encoding amine oxidases showed a net down-regulation in Tx7000. Thus, amine

298   oxidase-mediated apoplastic H_2O_2 production would remain minimal in the susceptible genotype

299   in response to *M. phaseolina* inoculation.

300

301   NADH dehydrogenases are a source of ROS production in mitochondria (Moller 2001; Arora et

302   al. 2002). The significant up-regulation of two NADH dehydrogenase genes (*Sb02g037780*,

303   *Sb03g033415*) suggested the potential contribution of mitochondria as a source of enhanced ROS

304   production in Tx7000 in response to pathogen inoculation. Consistent with the gene expression

305   data, the in vitro DCF-based ROS and RNS functional assay revealed *M. phaseolina*'s ability to

306   significantly increase the stalk free radicle content of both susceptible genotypes (BTx3042 and

307   Tx7000) at all three post inoculation stages (4, 7, and 10 DPI). Therefore, *M. phaseolina*'s ability

308   to trigger an oxidative stress response in charcoal rot susceptible sorghum genotypes was evident.

309

310   Along with ROS, NO plays a vital role in the hypersensitive response to avirulent biotrophic

311   pathogens (Delledonne et al. 1998; Durner et al. 1998; Yoshioka et al. 2011). The role of NO in

312   host defense against necrotrophs is contradictory. For instance, NO is claimed to confer resistance

313   against certain necrotrophic fungal pathogens (Asai et al. 2010; Perchepied et al. 2010). On the

314   contrary, an accumulation of NO in host tissue correlated with enhanced disease susceptibility was

315   observed in the compatible jute-*M. phaseolina* (Sarkar et al. 2014) and lily-*Botrytis*

316   *elliptica* interactions (van Baarlen et al. 2004). Agreeing with the latter phenomenon, we observed

317   an NO burst in susceptible sorghum stalk tissues (Tx7000, BTx3042) after *M. phaseolina*

318   inoculation. NO-specific fluorescence was found to be stronger in the vascular bundle regions. As

319   no mycelial fragments or microsclerotia were observed in the cross-sections, the observed NO was

320   exclusively from the host. If so, this suggests the systemic circulation of NO through the vascular

321   tissues. Moreover, fluorescence was observed in parenchyma cells, which indicated the cell-to-

322   cell movement of NO. The movement of NO via apoplastic and symplastic pathways has been

323   described (Graziano and Lamattina, 2005).

324

325   The RNA sequencing experiment provided some clues on the host metabolic pathways that

326   contributed to the surge in NO. The nitrate reduction I and citrulline-nitric oxide cycles are the

327   primary NO biosynthetic pathways in plants (Planchet and Kaiser 2006). In the citrulline-nitric

328   oxide cycle, NO is synthesized from arginine by nitric oxide synthase, generating L-citrulline as a

329   by-product (Planchet and Kaiser 2006). In the current study, the down-regulated nitric oxide

330   synthase genes in Tx7000 suggested that the citrulline-nitric oxide cycle remains inactive during

331   *M. phaseolina* infection and is not a significant source pathway for NO synthesis. Interestingly,

332   the genes encoding nitrite reductase (EC 1.7.2.1), which are involved in the nitrate reduction I

333   pathway were highly up-regulated in Tx7000 after pathogen inoculation. Nitrite reductase converts

334   nitrite into NO. Therefore, the nitrate reduction I pathway appeared to be the major source of host-

335   derived NO in response to *M. phaseolina* infection. This argument is further bolstered by the

336   observed down-regulation of the nitrate reduction II (assimilatory) pathway in Tx7000 after

337   pathogen inoculation. In this pathway, the Tx7000 genes encoding NADH-cytochrome b5

338   reductase (EC 1.7.1.1), which catalyzes the conversion of nitrate to nitrite, were down-regulated,

339   limiting nitrite to ammonia and ammonia to L-glutamine conversions in the chloroplast. Therefore,

340   the down-regulated NADH-cytochrome b5 reductase genes increase the availability of nitrate

341   pools for the nitrate reduction I pathway where nitrate is reduced to NO. Therefore, over-

342   accumulation of NO in the stalk tissues as induced by *M. phaseolina* appears to constitute a key

343   element in determining the success of this necrotrophic pathogen.

344

345   In the current study, evidence for NO and $O_2^{\bullet-}$ accumulation in charcoal rot susceptible sorghum

346   genotypes after *M. phaseolina* inoculation has been shown. NO can react with $O_2^{\bullet-}$ to form the

347   RNS species, peroxynitrite ($ONOO^-$) (Koppenol et al. 1992). Peroxynitrite triggers a myriad of

348   cytotoxic effects including lipid peroxidation, protein unfolding and aggregation, and DNA strand

349   breakage (Vandelle and Delledonne 2011; Murphy 1999). When produced abundantly, $ONOO^-$

350   contributes to rapid necrosis, whereas lower quantities induce apoptosis (Bonfoco et al. 1995).

351   Although not tested, the significantly increased free radical content observed in charcoal rot-

352   susceptible genotypes could be indicative of an increase in $ONOO^-$ in pathogen-inoculated Tx7000

353   and BTx3042. Therefore, plant-derived $ONOO^-$ may play a role as an endogenous virulence factor

354   for *M. phaseolina*.

355

356   ROS- and RNS-associated lipid peroxidation during pathogen infection has been widely described

357   (Jalloul et al. 2002; Göbel et al. 2003; Zoeller et al. 2012). The peroxidation of unsaturated fatty

358   acids in phospholipids produces malondialdehyde (MDA), which in turn damages cell and

359   organelles membranes (Halliwell and Gutteridge 1989). The oxidative stress experienced by

360   charcoal rot susceptible sorghum genotypes after *M. phaseolina* inoculation was further confirmed

361   by enhanced lipid peroxidation observed in those genotypes.

362

363   **Impact of *M. phaseolina* infection on the sorghum antioxidant system**

364

365   Activation of plant antioxidant systems in response to various pathogens and its contribution to

366   enhanced disease resistance has been well documented (Malencic et al. 2010; Kiprovski et al.

367   2012; Debona et al. 2012; Fortunato et al. 2015). On the contrary, the fungal necrotroph *Botrytis*

368   *cinerea* triggers a progressive inhibition of SOD, CAT, and PX parallel to disease symptom

369   development in tomato and leads to a collapse of the peroxisomal antioxidant system at advanced

370   stages of infection (Kuzniak and Sklodowska 2005). However, infection of the necrotrophic

371   fungus, *Corynespora cassiicola* enhanced peroxidase activity in soybean leaves (Fortunato et al.

372   2015). Gene expression (7 DPI) and the peroxidase functional experiment (4, 7, and 10 DPI)

373   conducted in the current study revealed a significant up-regulation of peroxidase activity in

374   charcoal rot susceptible genotypes after *M. phaseolina* inoculation. This suggested the enhanced

375   accumulation of H_2O_2 after infection. Peroxidases are antioxidant enzymes that convert toxic H_2O_2

376   into H_2O and O_2 (Hammond and Jones 1996). It appeared that increased peroxidase activity in

377   Tx7000 and BTx3042 helps to lower their H_2O_2 concentrations and thus reduce oxidative stress

378   after *M. phaseolina* infection.

379

380   Catalase is a key H_2O_2-scavenging enzyme in plants (Willekens et al. 1997) and has one of the

381   highest turnover rates for all enzymes where one molecule of catalase can convert six million

382   molecules of H_2O_2 to H_2O and O_2 min^{-1} (Gill and Tuteja 2010). In tobacco, reduced catalase

383   activity results in hyper-responsiveness to biotrophic pathogens (Mittler et al. 1999), while catalase

384   overexpression leads to enhanced disease sensitivity (Polidoros et al. 2001). Previous reports

385   revealed that catalase activity is suppressed during the interaction of plants with invading

386   pathogens and in turn, contributes to the escalation of pathogen-induced programmed cell death

387   (PCD) (Draper 1997; Chamnongpol et al. 1996; Chen et al. 1993; Takahashi et al. 1997).

388   Suppressed catalase activity-associated ROS production augmentation, is therefore crucial for

389   conferring resistance against biotrophic and hemibiotrophic plant pathogens while conducive to

390   necrotrophic infection. *M. phaseolina* inoculation leads to reduced catalase activity in two charcoal

391   rot-susceptible sorghum genotypes at 7 DPI. One potential reason for this observation is the

392   reaction between NO and catalase. NO and $ONOO^-$ can bind with heme-containing antioxidant

393   enzymes such as catalase and inhibit its activity (Kerwin et al. 1995; Pacher et al. 2007). NO is

394   produced in pathogen-inoculated Tx7000 and BTx3042 at 7 DPI and could, in turn, inhibit catalase

395   activity. Enhanced catalase activity in the two resistant genotypes after *M. phaseolina* inoculation

396   at all post-inoculation stages could contribute to active scavenging of H_2O_2 and ease oxidative

397   stress. This, in turn, could subvert *M. phaseolina* colonization in SC599 and SC35, which

398   contributes to resistance.

399

400   A significant reduction in superoxide dismutase activity was observed at 7 and 10 DPI by *M.*

401   *phaseolina* (compared to control) across the four genotypes tested in this study. Transcriptional

402   data suggested *M. phaseolina*'s ability to increase the $O_2{}^{\cdot-}$ biosynthesis potential of Tx7000. This,

403   arguably, increases the Tx7000's necessity for more SOD as it is the only plant enzyme capable

404   of scavenging $O_2{}^{\cdot-}$. However, by using confocal microscopy and the ROS/RNS functional assay,

405   evidence exists for potentially enhanced $ONOO^-$ synthesis in susceptible genotypes under

406 pathogen inoculation. Formation of $ONOO^-$ leads to decreased endogenous $O_2^{\cdot-}$ levels. Therefore,

407 it may be possible that $O_2^{\cdot-}$ decreases to a level where additional SOD is not required by the

408 susceptible genotypes tested. This manifested as reduced SOD activity after *M. phaseolina*

409 inoculation.

410

411 In this study, genome-wide transcriptome profiles of *M. phaseolina*-challenged charcoal rot

412 resistant (SC599) and susceptible (Tx7000) sorghum genotypes were examined to identify the

413 differentially expressed genes that related to host oxidative stress and antioxidant system. The

414 observed up-regulation of cytochrome P450s, which potentiate NAD(P)H-dependent $O_2^{\cdot-}$

415 production in the endoplasmic reticulum, and NADH dehydrogenase genes, respectively,

416 suggested the importance of endoplasmic reticulum and mitochondria as ROS generating

417 powerhouses that contributed to enhanced oxidative stress in Tx7000 after *M. phaseolina*

418 inoculation. Enhanced pathogen inoculation-mediated oxidative stress enhancement in Tx7000

419 and BTx3042 was confirmed by increased ROS/RNS and malondialdehyde content. Prominent

420 nitric oxide (NO) accumulation observed in Tx7000 and BTx3042 after *M. phaseolina* inoculation

421 was associated with the up-regulated host nitrate reduction I metabolic pathway. Transcriptional

422 and functional data demonstrated enhanced peroxidase and decreased catalase and superoxide

423 dismutase activities in inoculated susceptible genotypes. Overall, this study demonstrated the

424 ability of *M. phaseolina* to trigger strong host-derived oxidative stress in charcoal rot susceptible

425 sorghum genotypes. Host cell death associated with enhanced oxidative stress in turn contribute

426 to the rapid colonization and spread of this necrotrophic fungus leading to induced charcoal rot

427 susceptibility. Use of differentially expressed genes and *in planta* NO synthesis as potential

428 molecular- and biochemical-markers in sorghum germplasm screening for charcoal rot resistance

429 and susceptibility is of interest for future research.

430

431

432 **MATERIALS AND METHODS**

433

434 **Plant materials and experimental design**

435

436 Two greenhouse experiments were conducted to obtain materials for investigation. For the RNA-

437 Seq experiment, one charcoal rot resistant (SC599) and one susceptible (Tx7000) sorghum

438 genotype were used in 2013. In 2015, follow-up functional studies were conducted using charcoal

439 rot resistant (SC599, SC35) and susceptible (Tx7000, BTx3042) lines. For both greenhouse

440 experiments, seeds were treated with the fungicide Captan (N-trichloromethyl thio-4-cyclohexane-

441 1,2 dicarboxamide) and planted in 19 L Poly Tainer pots filled with Metro-Mix 360 growing

442 medium (Sun Gro Bellevue, WA, U.S.A). Although three seeds were planted pot^{-1} at the beginning

443 of each experiment, each pot was thinned to one seedling at three weeks after emergence.

444 Maintenance of seedlings and plants was performed according to the protocols described by

445 Bandara et al. (2015). Plants were maintained at 25 to 32°C under a 16-h light/8-h dark

446 photoperiod. Both greenhouse experiments were established as a completely randomized design

447 (CRD).

448

449 **Inoculum preparation and inoculation**

450

451   A highly virulent *M. phaseolina* isolate obtained from the Row Crops Pathology Lab at the

452   Department of Plant Pathology, Kansas State University was used for inoculation. Inoculum

453   preparation was based upon the protocol published by Bandara et al. (2015). Briefly, *M. phaseolina*

454   was grown for 5 d on potato dextrose agar (PDA) at 30°C. For the mass production of mycelia, *M.*

455   *phaseolina* cultures were initiated in potato dextrose broth (PDB) shake cultures. The broth

456   containing the mycelial mass was blended and filtered through four layers of sterile cheesecloth to

457   obtain small mycelial fragments. Filtrates with mycelial fragments were centrifuged at 3000 g for

458   five minutes. The mycelial pellets were resuspended in 50 mL of 10 mM (pH 7.2) sterile

459   phosphate-buffered saline (PBS; pH 7.2). The original mycelial fragment concentration was

460   determined using a hemocytometer and the final concentration was adjusted to 2×10^6 fragments

461   mL^{-1} by adding an appropriate volume of PBS. Inoculum preparation occurred under aseptic

462   conditions. Inoculations were performed at 14 d after anthesis. The plant basal internode was

463   injected with 0.1 mL of inoculum (1×10^6 viable mycelial fragments mL^{-1}) using a sterile surgical

464   syringe. Mock-inoculations (control treatment) were performed with PBS (pH 7.2).

465

466   **Collection of stalk tissues from inoculated plants**

467

468   Stalk tissues of inoculated and mock-inoculated control plants were collected from three biological

469   replicates at 2, 7, and 30 days post-inoculation (DPI) (three biological replicates DPI^{-1} treatment^{-1}

470   sorghum line^{-1} = 36 plants total) for the RNA sequencing experiment. From each biological

471   replicate, an approximately 8 to 10 cm long stalk piece encompassing the inoculation point was

472   collected and immediately frozen in liquid nitrogen to prevent mRNA degradation and then stored

473   at -80°C until RNA was extracted. At 4, 7, and 10 DPI, 15 cm long stalk pieces encompassing the

474   inoculation point were cut from five biologically replicated plants, immediately suspended in

475   liquid nitrogen, and subsequently stored at -80°C until used in functional assays.

476

477   **RNA extraction and quantification**

478

479   Stalk tissues (approximately 1 g) from 1 cm above the symptomatic area were used for RNA

480   extraction. Total RNA was extracted using Triazole reagent (Thermo Scientific, USA). RNA was

481   treated with Amplification Grade DNAse I (Invitrogen Corporation, USA). The quantity and

482   quality of RNA extracts were assessed using a Nanodrop 2000 (Thermo Scientific, USA). Samples

483   were diluted up to 100 to 200 ng/µl concentration using RNase-free water. Before cDNA library

484   preparation, the integrity and quantity of diluted RNA samples were reassessed using an Agilent

485   2100 Bioanalyzer (Agilent Technologies Genomics, USA) to ensure the quality of cDNA libraries.

486

487   **cDNA library preparation and Illumina sequencing**

488

489   Using the Illumina TruSeq^{TM} RNA sample preparation kit and the manufacturer's protocol

490   (Illumina Inc., USA), thirty-six cDNA libraries were constructed. First, using "oligodT" attached

491   magnetic beads, each RNA sample was subjected to two rounds of enrichment for poly-A mRNAs.

492   Purified mRNA was then chemically fragmented and then converted to single-stranded cDNA.

493   cDNA of each library was differentially barcoded using unique adapter index sequences.

494   Sequencing was conducted on a HiSeq 2000 platform (Illumina Inc., USA) using 100 bp single-

495   end sequencing runs at the Kansas University Medical Center Genome Sequencing Facility

496   (Lawrence, Kansas). These libraries were also used for differential analysis of host-induced cell

497   wall degrading enzyme genes in the *M. phaseolina*-sorghum pathosystem (Bandara et al., 2018b).

498

499   **Differential gene expression and metabolic pathway enrichment analyses**

500

501   First, trimming of adapters from sequence reads and subsequent quality filtering were carried out

502   using "Cutadapt" (Martin, 2011). GSNAP (genomic short-read nucleotide alignment program; Wu

503   and Watanabe, 2005) was used to align reads to the *Sorghum bicolor* reference genome

504   (Sbicolor_v1.4; Paterson et al., 2009). An R package, 'DESeq2', was used to perform the

505   differential gene expression analysis, where the analysis was based on the H_o of no two-way

506   interaction between sorghum line and inoculation treatment for each gene at a given DPI. A q-

507   value (Benjamini and Hochberg, 1995) was determined for each gene and those genes with q-

508   values < 0.05 were considered significantly differentially expressed (i.e., a significant two-way

509   interaction) to account for multiple comparisons. Therefore, the false discovery rate (FDR) was

510   maintained at 5%. The differentially expressed genes were annotated using the "Phytozome"

511   database (Goodstein et al., 2012). The metabolic pathways associated with differentially expressed

512   genes   were   identified   using   the   SorghumCyc   database   (http://pathway.

513   gramene.org/gramene/sorghumcyc.shtml). Finally, the significantly enriched metabolic pathways

514   were determined using metabolic pathway enrichment analysis as described by Dugas et al. (2011).

515

516   **Preparation of cell lysates and measuring absorption and fluorescence for functional assays**

517

518 Stalk tissues were retrieved from -80°C storage and approximately 1 g of stalk tissue (taken 1 cm

519 away from the symptomatic region) were sectioned and placed into liquid nitrogen (in a mortar)

520 using a sterile scalpel. The stalk pieces were ground into a fine powder using a pestle.

521 Approximately 200 mg of the tissue powder was quickly transferred to 2 mL microcentrifuge tubes

522 filled with 1 ml of $1\times$ PBS + 0.5% Triton X (for in vitro ROS/RNS assay), $1\times$ PBS with $1\times$ BHT

523 (for quantification of lipid peroxidation via the thiobarbituric acid reactive substances assay), $1\times$

524 PBS with 1mM EDTA (for the catalase and peroxidase assays), and $1\times$ lysis buffer (10 mM Tris,

525 pH 7.5, 150 mM NaCl, 0.1 mM EDTA; for superoxide dismutase assay). Buffer selections were

526 based on the instructions provided by assay kit manufacturers (see below). Samples were

527 centrifuged at 10000 g for 10 min at 4°C. Supernatants were transferred into new microcentrifuge

528 tubes and stored at -80°C until used in assays. All absorption and fluorescence were performed

529 using a 96-well plate reader (Synergy H1 Hybrid Reader; BioTek, Winooski, VT, USA) at

530 specified wavelengths (see below). Path length correction was performed using an option available

531 by the plate reader during the measurements.

532

533 **Quantification of total oxidative stress**

534

535 The OxiSelect In Vitro ROS/RNS Assay Kit (Cell Biolabs, San Diego, CA, USA) was used to

536 quantify reactive species (ROS) and reactive nitrogen species (RNS) content. The assay employs

537 a ROS/RNS-specific fluorogenic probe, dichlorodihydrofluorescein DiOxyQ (DCFH-DiOxyQ),

538 which is first primed with a quench removal reagent and subsequently stabilized in the highly

539 reactive DCFH form. Various ROS and RNS such as hydrogen peroxide (H_2O_2), peroxyl radical

540 (ROO·), nitric oxide (NO), and the peroxynitrite anion ($ONOO^-$) can react with DCFH and oxidize

541   it into the fluorescent 2′,7′-dichlorodihydrofluorescein (DCF) molecule. Fluorescence intensity is

542   proportional to the ROS and RNS content within the sample. The assay measures the total free

543   radical population within a sample. In this study, reactive species content was assayed following

544   the protocol described by the manufacturer. Briefly, 50 μL of the supernatant (see the previous

545   section) from each sample was transferred to a black 96-well Nunclon Delta Surface microplate

546   (Thermo Scientific Nunc, Roskilde, Denmark) and incubated with the catalyst (1×) for 5 min at

547   room temperature. One hundred μL of freshly prepared DCFH solution was added to each well

548   and incubated for 45 min. The reaction mix was protected from light using aluminum foil. After

549   incubation, sample fluorescence was measured at 485 nm excitation and 535 nm emission

550   wavelengths. A dilution series of DCF standards (in the concentration range of 0 to 10 μM) was

551   prepared by diluting the 1mM DCF stock in 1× PBS and then used to prepare a DCF standard

552   curve. Sample reactive species were determined using a DCF standard curve and expressed as mM

553   DCF 200 mg^{-1} fresh stalk tissue.

554

555   **Detection of nitric oxide (NO) by confocal microscopy**

556

557   A cell-permeable fluorescent dye, 4-amino-5-methylamino-2',7'-difluorofluorescein diacetate

558   (DAF-FM DA; Molecular Probes, Eugene, OR, USA) was used to detect NO production in

559   sorghum genotype stalks in response to inoculation treatment at 7 DPI. DAF-FM DA is non-

560   fluorescent until it reacts with NO to form DAF-FM (bright green fluorescence). The fluorescence

561   quantum yield of DAF-FM increases about 160-fold after reacting with nitric oxide (Kojima et al.,

562   1999). In this study, sorghum stem cross sections (made 1 cm away from the symptomatic area)

563   were incubated with 10 mM DAF-FM DA prepared in 10 mM Tris-HCl (pH 7.4) for 1 h at 25 C,

564   in the dark (Corpas et al., 2004). After incubation, samples were washed twice with 10 mM Tris-

565   HCl buffer for 15 min each. Tissue sections were examined using a Carl Zeiss 700 confocal

566   microscope. Light intensity and exposure times were constant across all observations. DAF-FM

567   DA fluorescence (excitation 495 nm; emission 515 nm) and chlorophyll *a* and *b* autofluorescence

568   (excitation 329 and 450 nm; emission 650 and 670 nm) registered as green and red, respectively.

569   For each sorghum genotype, the fluorescence of the mock-inoculated treatment (control) was used

570   as the baseline.

571

572   **Quantification of peroxidase activity**

573

574   The Amplex Red Hydrogen Peroxide/Peroxidase Assay Kit (Molecular Probes, Eugene, OR,

575   USA) was used for peroxidase activity determination. In the presence of peroxidase, the Amplex

576   Red reagent reacts with H_2O_2 in a 1:1 stoichiometry to produce the red-fluorescent oxidation

577   product, resorufin. In this study, 50 μL of the sample was diluted in a microcentrifuge tube by

578   adding 200 μL of 1× reaction buffer. Fifty μL from each diluted sample was transferred to a black

579   96-well microplate. Then, 50 μL of the Amplex Red reagent/H_2O_2 working solution (100 μM

580   Amplex Red reagent containing 2 mM H_2O_2) was added. The microplate was covered with

581   aluminum foil to protect from light and was incubated at room temperature for 30 minutes.

582   Fluorescence was read at 545 nm excitation and 590 nm emission detection. Blanks included every

583   component mentioned above in which 50 μL 1× reaction buffer was added in place of peroxidase.

584   For each point, the value derived from the control was subtracted. A horseradish peroxidase (HRP)

585   standard curve was prepared by following the protocol described by the assay kit manufacturer.

586   The peroxidase activity of samples was determined using the HRP standard curve and expressed

587   as milliunits of peroxidase mL^{-1} 200 mg^{-1} of fresh stalk tissue where 1 U of enzyme forms 1.0 mg

588   purpurogallin from pyrogallol 20 sec^{-1} at pH 6.0 at 20°C.

589

590   **Quantification of catalase activity**

591

592   Catalase activity was determined using the OxiSelect Catalase Activity Assay Kit (Cell Biolabs,

593   San Diego, CA, USA). The kit assay involves catalase induced decomposition of externally

594   introduced H_2O_2 into water and oxygen. The rate of this decomposition is proportional to the

595   catalase concentration in the sample. In the presence of horseradish peroxidase (HRP) catalyst, the

596   remaining hydrogen peroxide in the reaction mixture facilitates the coupling reaction of the two

597   chromagens used in the assay, forming a quinoneimine dye. Absorption of this dye is measured at

598   520 nm. The absorption is proportional to the amount of hydrogen peroxide remaining in the

599   reaction mixture, which is indicative of the original catalase activity of the sample. In this study,

600   20 μL of the sample was transferred to a clear 96-well microtiter plate. Fifty μL of a hydrogen

601   peroxide working solution (12 mM) was added to each well, thoroughly mixed, and incubated for

602   1 min. The reaction was stopped by adding 50 μL of the catalase quencher into each well and

603   mixed. Five μL of each reaction well was transferred to a new 96-well microtiter plate. Two-

604   hundred-fifty μL of chromogenic working solution was added to each well. The plate was

605   incubated for 1 hour with vigorous mixing on a shaker (140 rotations min^{-1}). Absorbance was

606   measured at 520 nm. A catalase standard curve was prepared by following the protocol described

607   by the assay kit manufacturer. The catalase activity of the samples was determined using the

608   standard curve and expressed as units of catalase mL^{-1} 200 mg^{-1} of fresh stalk tissue where 1 unit

609   (U) is defined as the amount of enzyme that will decompose 1.0 µmole of H_2O_2 min^{-1} at pH 7.0

610   and 25°C.

611

612   **Quantification of superoxide dismutase (SOD) activity**

613

614   The OxiSelect Superoxide Dismutase Activity Assay kit (Cell Biolabs, San Diego, CA, USA) was

615   used to quantify SOD activity. This assay uses a xanthine/xanthine oxidase (XOD) system to

616   generate superoxide anions. Upon reduction by superoxide anions, the assay chromagen produces

617   a formazan dye that is soluble in water. SOD activity is computed as the inhibition of chromagen

618   reduction. Therefore, in the presence of SOD, superoxide anion concentrations are reduced,

619   resulting in a weak colorimetric signal. In the current study, 20 µL from each sample was

620   transferred to a 96-well microtiter plate. According to the kit manufacturer's protocol, each well

621   contained xanthine solution (5 µL, 1×), chromogen solution (5 µL), SOD assay buffer (10 µL,

622   10×), and distilled water (50 µL). Finally, 10 µL of xanthine oxidase solution (1×) was added to

623   each well and mixed well. Blank tests included every component mentioned above except 20 µL

624   of 1× lysis buffer instead of the SOD sample. After 1 hour of incubation at 37°C, absorbance was

625   read at 490 nm. SOD activity was computed using the formula below:

626

627   SOD activity (% inhibition) = [(OD_{blank} - OD_{sample}) ÷ OD_{blank}] × 100

628

629   **Quantification of lipid peroxidation**

630

631   To estimate lipid peroxidation stalk sample malondialdehyde (MDA) content was measured using

632   a TBARS (thiobarbituric acid reactive substances) assay kit (OxiSelect; Cell Biolabs, San Diego,

633   CA, USA). Cellular oxidative stress results in the production of unstable lipid peroxides, which

634   decompose into products such as MDA (Kappus, 1985). The TBARS assay is based on MDA's

635   reactivity with thiobarbituric acid (TBA) via an acid-catalyzed nucleophilic-addition reaction. The

636   fluorescent 1 MDA:2 TBA adduct that results from the above reaction has an absorbance

637   maximum at 532 nm and can be measured calorimetrically (Kappus, 1985; Janero, 1990). The one-

638   hundred μL of sample was incubated with 100 μL of sodium dodecyl sulfate lysis solution in a

639   microcentrifuge tube for 5 min at room temperature. Thiobarbituric acid (250 μL) was added to

640   each sample and incubated at 95°C for 1 h. After cooling to room temperature on ice for 5 min,

641   samples were centrifuged at 3000 rpm for 15 min. The supernatant (200 μL) was transferred to a

642   96-well microplate, and the absorbance was read at 532 nm. A dilution series of MDA standards

643   (in the concentration range of 0 to 125 μM) was prepared by diluting the MDA standard in

644   deionized water and used to prepare a standard curve. MDA content of the samples was determined

645   and expressed as μmol 200 mg^{-1} of stalk tissue (fresh weight).

646

647   **Statistical analysis of functional assay data**

648

649   The PROC GLIMMIX procedure of SAS software version 9.2 (SAS Institute, 2008) was used to

650   analyze the functional ROS/RNS assay, peroxidase activity, catalase activity, SOD activity, and

651   lipid peroxidation assay data for variance (ANOVA). Variance components for two fixed factors,

652   genotype, and inoculation treatment, were estimated using the restricted maximum likelihood

653   (REML) method at each post-inoculation stage (4, 7, and 10 DPI). The assumptions of identical

654   and independent distribution of residuals and their normality were tested using studentized residual

655   plots and Q-Q plots, respectively. Whenever residuals were not homogenously distributed,

656   appropriate heterogeneous variance models were fitted to meet the model assumptions. For this, a

657   random/group statement (group = genotype or inoculation treatment) was specified after the model

658   statement. The most parsimonious model was selected using Bayesian information criterion (BIC).

659   Means were separated using the PROC GLMMIX procedure of SAS. Main effects of factors were

660   determined using the Tukey-Kramer test with the adjustments for multiple comparisons. The

661   simple effects of the inoculation treatment were determined at each genotype level (four

662   genotypes), whenever genotype × treatment interaction was statistically significant. As inoculation

663   treatment comprised only two levels (control and *M. phaseolina*), there was no a need to adjust the

664   critical *P*-values for multiple comparisons.

665

666

667   **ACKNOWLEDGEMENTS**

668

674

675

676

677   **LITERATURE CITED**

678

679   1. Allan, A. C., and Fluhr, R. 1997. Two distinct sources of elicited reactive oxygen species

680   in tobacco epidermal cells. Plant Cell 9:1559-1572.

681

682   2. Aly, A. A., Abdel-Sattar, M. A., Omar, M. R., and Abd-Elsalam, K. A. 2007. Differential

683   antagonism of *Trichoderma* sp. against *Macrophomina phaseolina*. J Plant Prot Res. 47:91-

684   102.

685

686   3. Arora, A., Sairam, R. K., and Srivastava, G. C. 2002. Oxidative stress and antioxidative

687   system in plants. Curr. Sci. 82:1227-1238.

688

689   4. Asai, S., Mase, K., and Yoshioka, H. 2010. Role of nitric oxide and reactive oxygen species

690   in disease resistance to necrotrophic pathogens. Plant Signal Behav. 5:872-874.

691

692   5. Auh, C. K., and Murphy, T. M. 1995. Plasma membrane redox enzyme is involved in the

693   synthesis of O_2^- and H_2O_2 by *Phytophthora* elicitor-stimulated rose cells. Plant Physiol.

694   107: 1241-1247.

695

696   6. Bandara, Y. M. A. Y., Tesso, T. T., Zhang, K., Wang, D., and Little, C. R. 2018a. Charcoal

697   rot and Fusarium stalk rot diseases influence sweet sorghum sugar attributes. Ind. Crops

698   Prod. 112:188-195.

699

700   7. Bandara, Y.M.A.Y., Weerasooriya, D.K., Liu, S. and Little, C.R., 2018b. The necrotrophic

701   fungus *Macrophomina phaseolina* promotes charcoal rot susceptibility in grain sorghum

702   through induced host cell wall-degrading enzymes. Phytopathology 108:948-956.

703

704   8. Bandara, Y. M. A. Y., Tesso, T. T., Bean, S. R., Dowell, F. E., and Little, C. R. 2017a.

705   Impacts of fungal stalk rot pathogens on physicochemical properties of sorghum grain.

706   Plant Dis. 101:2059-2065.

707

708   9. Bandara, Y. M. A. Y., Weerasooriya, D. K., Tesso, T. T., Prasad, P.V.V., and Little, C. R.

709   2017b. Stalk rot fungi affect grain sorghum yield components in an inoculation stage-

710   specific manner. Crop prot. 94:97-105.

711

712   10. Bandara, Y. M. A. Y., Weerasooriya, D. K., Tesso, T. T., and Little, C. R. 2017c. Stalk rot

713   diseases impact sweet sorghum biofuel traits. BioEnergy Res. 10:26-35.

714

715   11. Bandara, Y. M. A. Y., Weerasooriya, D. K., Tesso, T. T., and Little, C. R. 2016. Stalk Rot

716   Fungi affect leaf greenness (SPAD) of grain sorghum in a genotype-and growth-stage-

717   specific manner. Plant Dis. 100:2062-2068.

718

719   12. Bandara, Y. M. A. Y., Perumal, R., and Little, C. R. 2015. Integrating resistance and

720   tolerance for improved evaluation of sorghum lines against Fusarium stalk rot and charcoal

721   rot. Phytoparasitica 43:485-499.

722

723   13. Benjamini, Y., and Hochberg, Y. 1995. Controlling the false discovery rate: a practical and

724   powerful approach to multiple testing. J R Stat Soc Series B Stat Methodol. 57: 289-300.

725

726   14. Bhattacharya, D., Dhar, T. K., and Ali, E. 1992. An enzyme immunoassay of phaseolinone

727   and its application in estimation of the amount of toxin in *Macrophomina phaseolina*-

728   infected seeds. Appl. Environ. Microbiol. 77:1970-1974.

729

730   15. Bonfoco, E., Krainc, D., Ankarcrona, M., Nicotera, P., and Lipton, S. A. 1995. Apoptosis

731   and necrosis: two distinct events induced, respectively, by mild and intense insults with

732   Nmethyl- D-aspartate or nitric oxide/superoxide in cortical cell cultures. Proc. Natl. Acad.

733   Sci. U.S.A. 92:7162-7166.

734

735   16. Chamnongpol, S., Willekens, H., Langebartels, C., Van Montagu, M., Inzé, D., and Van

736   Camp, W. 1996. Transgenic tobacco with a reduced catalase activity develops necrotic

737   lesions and induces pathogenesis-related expression under high light. Plant J. 10:491-503.

738

739   17. Choquer, M., Fournier, E., Kunz, C., Levis, C., Pradier, J. M., Simon, A., and Viaud, M.

740   2007. *Botrytis cinerea* virulence factors: new insights into a necrotrophic and

741   polyphageous pathogen. FEMS Microbiol Lett. 277:1-10.

742

743   18. Chen, Z., Silva, H., and Klessig, D. F. 1993. Active oxygen species in the induction of

744   plant systemic acquired resistance by salicylic acid. Science 262:1883-1886.

745

746   19. Cona, A., Rea, G., Angelini, R., Federico, R., and Tavladoraki, P. 2006. Functions of amine

747   oxidases in plant development and defense. Trends Plant Sci. 11:80-88.

748

749   20. Corpas, F.J., Barroso, J.B., Carreras, A., Quirós, M., León, A.M., Romero-Puertas, M.C.,

750   Esteban, F.J., Valderrama, R., Palma, J.M., Sandalio, L.M. and Gómez, M. 2004. Cellular

751   and subcellular localization of endogenous nitric oxide in young and senescent pea plants.

752   Plant Physiol. 136:2722-2733.

753

754   21. Dangl, J. L., and Jones, J. D. G. 2001. Plant pathogens and integrated defence responses to

755   infection. Nature 411:826-833.

756

757   22. De, B. K., Chattopadhya, S. B., and Arjunan, G. 1992. Effect of potash on stem rot diseases

758   of jute caused by *Macrophomina phaseolina*. J Mycopathol Res. 30: 51-55.

759

760   23. Debona, D., Rodrigues, F. Á., Rios, J. A., and Nascimento, K. J. T. 2012. Biochemical

761   changes in the leaves of wheat plants infected by *Pyricularia oryzae*. Phytopathology 102:

762   1121-1129.

763

764   24. Delledonne, M., Zeier, J., Marocco, A., and Lamb, C. 2001. Signal interactions between

765   nitric oxide and reactive oxygen intermediates in the plant hypersensitive disease resistance

766   response. Proc. Natl. Acad. Sci. U.S.A. 98:13454-13459.

767

768   25. Delledonne, M., Xia, Y., Dixon, R. A., and Lamb, C. 1998. Nitric oxide functions as a

769   signal in plant disease resistance. Nature 394: 585-588.

770

771   26. Doke, N. 1983. Involvement of superoxide anion generation in the hypersensitive response

772   of potato tuber tissues to infection with an incompatible race of *Phytophthora infestans* and

773   to the hyphal wall components. Physiol Mol Plant Pathol. 23:345-357.

774

775   27. Draper, J. 1997. Salicylate, superoxide synthesis and cell suicide in plant defense. Trends

776   Plant Sci. 2:162-165.

777

778   28. Dugas, D. V., Monaco, M. K., Olsen, A., Klein, R. R., Kumari, S., Ware, D., and Klein, P.

779   E. 2011. Functional annotation of the transcriptome of *Sorghum bicolor* in response to

780   osmotic stress and abscisic acid. BMC Genomics 12: 514.

781

782   29. Durner, J., Wendehenne, D. and Klessig, D. F. (1998). Defense gene induction in tobacco

783   by nitric oxide, cyclic GMP, and cyclic ADP-ribose. Proc. Natl. Acad. Sci. U.S.A.

784   95:10328-10333.

785

786   30. Edmunds, L. 1964. Combined relation of plant maturity temperature soil moisture to

787   charcoal stalk rot development in grain sorghum. Phytopathology 54: 513-517.

788

789   31. Foley, R. C., Kidd, B. N., Hane, J. K., Anderson, J. P., and Singh, K. B. 2016. Reactive

790   oxygen species play a role in the infection of the necrotrophic fungi, *Rhizoctonia solani* in

791   wheat. PloS One 11: e0152548.

792

793   32. Fortunato, A. A., Debona, D., Bernardeli, A. M. A., and Rodrigues, F. Á. 2015. Changes

794   in the antioxidant system in soybean leaves infected by *Corynespora cassiicola*.

795   Phytopathology 105:1050-1058.

796

797   33. Gill, S. S. and Tuteja, N. 2010. Reactive oxygen species and antioxidant machinery in

798   abiotic stress tolerance in crop plants. Plant Physiol Biochem. 48:909-930.

799

800   34. Göbel, C., Feussner, I., and Rosahl, S. 2003. Lipid peroxidation during the hypersensitive

801   response in potato in the absence of 9-lipoxygenases. J Biol Chem. 278: 52834-52840.

802

803   35. Goodstein, D.M., Shu, S., Howson, R., Neupane, R., Hayes, R.D., Fazo, J., Mitros, T.,

804   Dirks, W., Hellsten, U., Putnam, N., and Rokhsar, D.S. 2012. Phytozome: a comparative

805   platform for green plant genomics. Nucleic Acids Res. 40:1178-1186.

806

807   36. Govrin, E., and Levine, A. 2000. The hypersensitive response facilitates plant infection by

808   the necrotrophic pathogen *Botrytis cinerea*. Curr Biol. 10:751-757.

809

810   37. Grant, M., Brown, I., Adams, S., Knight, M., Ainslie, A., and Mansfield, J. 2000. The

811   RPM1 plant disease resistance gene facilitates a rapid and sustained increase in cytosolic

812   calcium that is necessary for the oxidative burst and hypersensitive cell death. Plant J.

813   23:441-450.

814

815   38. Graziano, M., and Lamattina, L. 2005. Nitric oxide and iron in plants: an emerging and

816   converging story. Trends Plant Sci. 10:4-8.

817

818   39. Halliwell, B., and Gutteridge, J. M. C. 1989. Free Radicals in Biology and Medicine (2nd

819   ed.). Oxford, UK: Clarendon.

820

821   40. Hammond-Kosack, K. E., and Jones, J. D. 1996. Resistance gene-dependent plant defense

822   responses. Plant Cell 8:1773-1791.

823

824   41. Hundekar, A., and Anahosur, K. 2012. Pathogenicity of fungi associated with sorghum

825   stalk rot. Karnataka Journal of Agricultural Sciences 7: 291-295.

826

827   42. Islam, M. S., Haque, M. S., Islam, M. M., Emdad, E. M., Halim, A., Hossen, Q. M. M.,

828   Hossain, M. Z., Ahmed, B., Rahim, S., Rahman, M. S., and Alam, M. M. 2012. Tools to

829   kill: Genome of one of the most destructive plant pathogenic fungi *Macrophomina*

830   *phaseolina*. BMC Genomics 13:493.

831

832   43. Jalloul, A., Montillet, J. L., Assigbetsé, K., Agnel, J. P., Delannoy, E., Triantaphylides, C.,

833   and Nicole, M. 2002. Lipid peroxidation in cotton: *Xanthomonas* interactions and the role

834   of lipoxygenases during the hypersensitive reaction. Plant J. 32:1-12.

835

836   44. Janero, D. R. 1990. Malondialdehyde and thiobarbituric acid-reactivity as diagnostic

837   indices of lipid peroxidation and peroxidative tissue injury. Free Radic Biol Med. 9:515-

838   540.

839

840   45. Jones, J. D., and Dangl, J. L. 2006. The plant immune system. Nature 444:323-329.

841

842   46. Kappus, H. 1985. Lipid peroxidation: mechanisms, analysis, enzymology and biological

843   relevance. Pages 273-310 in: *Oxidative stress*. H. Sies, ed. Academic Press London, UK.

844

845   47. Karuppanapandian, T., Moon, J. C., Kim, C., Manoharan, K., and Kim, W. 2011. Reactive

846   oxygen species in plants: their generation, signal transduction, and scavenging

847   mechanisms. Aust J Crop Sci. 5:709-725.

848

849   48. Kerwin, J. F., Lancaster, J. R., and Feldman, P. L. 1995. Nitric oxide: a new paradigm for

850   second messengers. J Med Chem. 38:4343-4362.

851

852   49. Kim, H. J., Chen, C., Kabbage, M., and Dickman, M. B. 2011. Identification and

853   Characterization of *Sclerotinia sclerotiorum* NADPH Oxidases. Appl Environ Microbiol.

854   77:7721-7729.

855

856   50. Kimber, C. T., Dahlberg, J. A., and Kresovich, S. 2013. The gene pool of *Sorghum bicolor*

857   and its improvement. Pages 23-41 in: *Genomics of the Saccharinae.* A.H. Paterson, ed.

858   Springer, New York.

859

860   51. Kiprovski, B., Malencic, D., Popovic, M., Budakov, D., Stojšin, V., and Baleševic-Tubic,

861   S. 2012. Antioxidant systems in soybean and maize seedlings infected with *Rhizoctonia*

862   *solani*. J Plant Pathol. 94:313-324.

863

864   52. Kliebenstein, D. J., and Rowe, H. C. 2008. Ecological costs of biotrophic versus

865   necrotrophic pathogen resistance, the hypersensitive response and signal transduction.

866   Plant Sci.174: 551-556.

867

868   53. Kojima, H., Urano, Y., Kikuchi, K., Higuchi, T., Hirata, Y., and Nagano, T. 1999.

869   Fluorescent indicators for imaging nitric oxide production. Angew Chem Int Ed. 38:3209-

870   3212.

871

872   54. Koppenol, W. H., Moreno, J. J., Pryor, W. A., Ischiropoulos, H., and Beckman, J. S. 1992.

873   Peroxynitrite, a cloaked oxidant formed by nitric oxide and superoxide. Chem Res Toxicol.

874   5:834-842.

875

876   55. Kużniak, E., and Skłodowska, M. 2005. Fungal pathogen-induced changes in the

877   antioxidant systems of leaf peroxisomes from infected tomato plants. Planta 222:192-200.

878

879   56. Malenčić, D., Kiprovski, B., Popović, M., Prvulović, D., Miladinović, J., and Djordjević,

880   V. 2010. Changes in antioxidant systems in soybean as affected by *Sclerotinia sclerotiorum*

881   (Lib.) de Bary. Plant Physiol Biochem. 48:903-908.

882

883   57. Martin, M. 2011. Cutadapt removes adapter sequences from high-throughput sequencing

884   reads. EMBnet J. 17:10-12.

885

886   58. Mayek-Pérez, N., López-Castañeda, C., López-Salinas, E., Cumpián-Gutiérrez, J., and

887   Acosta-Gallegos, J. A. 2001. *Macrophomina phaseolina* resistance in common bean under

888   field conditions in Mexico. Agrociencia 46:649-661.

889

890   59. Mittler, R. 2002. Oxidative stress, antioxidants and stress tolerance. Trends Plant Sci. 7:

891   405-410.

892

893   60. Mittler, R., Herr, E. H., Orvar, B. L., van Camp, W., Wilikens, H., Inzé, D, and Ellis, B. E.

894   1999. Transgenic tobacco plants with reduced capability to detoxify reactive oxygen

895   intermediates are hyperresponsive to pathogen infection. Proc. Natl. Acad. Sci. U.S.A. 96:

896   14165-14170.

897

898   61. Moller, I. M. 2001. Plant mitochondria and oxidative stress: Electron transport, NADPH

899   turnover, and metabolism of reactive oxygen species. Annu Rev Plant Physiol Plant Mol

900   Biol. 52:561-591.

901

902   62. Murphy, M. P. 1999. Nitric oxide and cell death. BBA-Bioenergetics 1411:401-414.

903

904   63. Nebert, D. W., Roe, A. L., Dieter, M. Z., Solis, W. A., Yang, Y., and Dalton, T. P. 2000.

905   Role of the aromatic hydrocarbon receptor and [*Ah*] gene battery in the oxidative stress

906   response, cell cycle control, and apoptosis. Biochem Pharmacol. 59:65-85.

907

908   64. Pacher, P., Beckman, J.S., and Liaudet, L. 2007. Nitric oxide and peroxynitrite in health

909   and disease. Physiol Rev. 87:315-424.

910

911   65. Paterson, A.H., Bowers, J.E., Bruggmann, R., Dubchak, I., Grimwood, J., Gundlach, H.,

912   Haberer, G., Hellsten, U., Mitros, T., Poliakov, A. and Schmutz, J. 2009. The *Sorghum*

913   *bicolor* genome and the diversification of grasses. Nature 457:551-556.

914

915   66. Perchepied, L., Balagué, C., Riou, C., Claudel-Renard, C., Rivière, N., Grezes-Besset, B.,

916   and Roby, D. 2010. Nitric oxide participates in the complex Interplay of defense-related

917   signaling pathways controlling disease resistance to *Sclerotinia sclerotiorum* in

918   *Arabidopsis thaliana*. Mol Plant Microbe Interact. 23:846-860.

919

920   67. Planchet, E., and Kaiser, W. M. 2006. Nitric oxide production in plants: facts and fictions.

921   Plant Signal Behav. 1:46-51.

922

923   68. Polidoros, A. N., Mylona, P. V., and Scandalios, J. P. 2001. Transgenic tobacco plants
924   expressing the maize *Cat2* gene have altered catalase levels that affect plant-pathogen
925   interactions and resistance to oxidative stress. Transgenic Res. 10:555-569.

926

927   69. Raguchander, T., Samiyappan, R., and Arjunan, G. 1993. Biocontrol of *Macrophomina*
928   root rot of mungbean. Indian Phytopath. 46:379-382.

929

930   70. Rosenow, D., Quisenberry, J., Wendt, C., and Clark, L. 1983. Drought tolerant sorghum
931   and cotton germplasm. Agric Water Manag. 7:207-222.

932

933   71. Sagi, M., and Fluhr, R. 2006. Production of reactive oxygen species by plant NADPH
934   oxidases. Plant Physiol. 141:336-340.

935

936   72. Sagi, M., and Fluhr, R. 2001. Superoxide production by plant homologues of the gp91phox
937   NADPH oxidase. Modulation of activity by calcium and by tobacco mosaic virus infection.
938   Plant Physiol. 126:1281-1290.

939

940   73. Sarkar, T. S., Biswas, P., Ghosh, S. K., and Ghosh, S. 2014. Nitric oxide production by
941   necrotrophic pathogen *Macrophomina phaseolina* and the host plant in charcoal rot disease
942   of jute: Complexity of the interplay between necrotroph–host plant interactions. PloS One
943   9: e107348.

944

945   74. Segmueller, N., Kokkelink, L., Giesbert, S., Odinius, D., van Kan, J., and Tudzynski, P.

946   2008. NADPH Oxidases are involved in differentiation and pathogenicity in *Botrytis*

947   *cinerea*. Mol Plant Microbe Interact. 21:808-819

948

949   75. Sharma, P., Jha, A. B., Dubey, R. S., and Pessarakli, M. 2012. Reactive oxygen species,

950   oxidative damage, and antioxidative defense mechanism in plants under stressful

951   conditions. Journal of Botany 2012:1-22.

952

953   76. Shetty, N. P., Jorgensen, H. J. L., Jensen, J. D., Collinge, D. B., and Shetty, H. S. 2008.

954   Roles of reactive oxygen species in interactions between plants and pathogens. Eur J Plant

955   Pathol. 121:267-280.

956

957   77. Stone, J. K. 2001. Necrotrophs. Encyclopedia of Plant Pathology 2:676-677.

958

959   78. Su, G., Suh, S. O., Schneider, R. W., and Russin, J. S. 2001. Host Specialization in the

960   Charcoal Rot Fungus, *Macrophomina phaseolina*. Phytopathology 91:120-126.

961

962   79. Takahashi, H., Chen, Z., Du, H., Liu, Y., and Klessig, D. F. 1997. Development of necrosis

963   and activation of disease resistance in transgenic tobacco plants with severely reduced

964   catalase levels. Plant J. 11:993-1005.

965

966   80. Tarr, S. A. J. 1962. Root and stalk diseases: Red stalk rot, Colletotrichum rot, anthracnose,

967   and red leaf spot. Pages 58-73 in: Diseases of Sorghum, Sudan Grass and Brown Corn.

968   Commonwealth Mycological Institute, Kew, Surrey, UK.

969

970   81. Tesso, T., Perumal, R., Little, C. R., Adeyanju, A., Radwan, G. L., Prom, L. K., and Magill,

971   C. W. 2012. Sorghum pathology and biotechnology-a fungal disease perspective: Part II.

972   Anthracnose, stalk rot, and downy mildew. Eur J Plant Sci Biotechnol. 6: 31-44.

973

974   82. Torres, M. A., Dangl, J. L., and Jones, J. D. G. 2002. *Arabidopsis* gp91[phox] homologues

975   *AtrbohD* and *AtrbohF* are required for accumulation of reactive oxygen intermediates in

976   the plant defense response. Proc. Natl. Acad. Sci. U.S.A 99:517-522.

977

978   83. Troy, C. M., Derossi, D., Prochiantz, A., Greene, L. A., and Shelanski, M. L. 1996.

979   Downregulation of Cu/Zn superoxide dismutase leads to cell death via the nitric oxide-

980   peroxynitrite pathway. J Neurosci. 16:253-261.

981

982   84. Vanacker, H., Carver, T. L., and Foyer, C. H. 2000. Early H_2O_2 accumulation in mesophyll

983   cells leads to induction of glutathione during the hyper-sensitive response in the barley-

984   powdery mildew interaction. Plant Physiol. 123:1289-1300.

985

986   85. Vandelle, E., and Delledonne, M. 2011. Peroxynitrite formation and function in plants.

987   Plant Sci. 181:534-539.

988

989 86. van Baarlen, P., Staats, M., and van Kan, J. A. L. 2004. Induction of programmed cell death

990   in lily by the fungal pathogen *Botrytis elliptica*. Mol Plant Pathol. 5:559-574.

991

992 87. van Kan, J. A. 2006. Licensed to kill: the lifestyle of a necrotrophic plant pathogen. Trends

993   Plant Sci. 11:247-253.

994

995 88. Willekens, H., Chamnongpol, S., Davey, M., Schraudner, M., Langebartels, C., Van

996   Montagu, M., Inzé, D. and Van Camp, W. 1997. Catalase is a sink for H_2O_2 and is

997   indispensable for stress defence in C3 plants. EMBO J. 16:4806-4816.

998

999 89. Wimalasekera, R., Tebartz, F., and Scherer, G. F. 2011. Polyamines, polyamine oxidases

1000   and nitric oxide in development, abiotic and biotic stresses. Plant Sci.181:593-603.

1001

1002 90. Wu, T.D., and Watanabe, C.K. 2005. GMAP: a genomic mapping and alignment program

1003   for mRNA and EST sequences. Bioinformatics 21:1859-1875.

1004

1005 91. Wyllie, T. D. 1998. Soybean Diseases of the North Central Region. Pages 106-113 in:

1006   Charcoal Rot of Soybean-Current Status. T. D. Wyllie and D. H. Scott, eds. American

1007   Phytopathological Society, St. Paul, MN.

1008

1009 92. Yang, S. L., and Chung, K. R. 2012. The NADPH oxidase-mediated production of

1010   hydrogen peroxide (H_2O_2) and resistance to oxidative stress in the necrotrophic pathogen

1011   *Alternaria alternata* of citrus. Mol Plant Pathol. 13:900-914.

1012

1013   93. Yoshioka, H., Mase, K., Yoshioka, M., Kobayashi, M., and Asai, S. 2011. Regulatory

1014   mechanisms of nitric oxide and reactive oxygen species generation and their role in plant

1015   immunity. Nitric Oxide 25:216-221.

1016

1017 **Table 1.** *P*-values of F-statistic from analysis of variance (ANOVA) for reactive oxygen/nitrogen

1018 species (ROS/RNS), peroxidase activity (PX), catalase activity (CAT), superoxide dismutase

1019 activity (SOD), and TBARS assay for malondialdehyde content measured at 4, 7, and 10 days post

1020 inoculation (DPI). All assays were based on cell extracts isolated from charcoal rot resistant

1021 (SC599, SC35) and susceptible (Tx7000, BTx3042) sorghum genotypes after inoculation with

1022 *Macrophomina phaseolina* and phosphate buffered saline (mock-inoculated control) ($\alpha = 0.05$).

1023

DPI	Effect	Pr > F				
		ROS/RNS	PX	CAT	SOD	TBARS
4	Genotype	0.0279	<0.0001	0.0002	0.0151	0.0024
	Treatment	0.0081	<0.0001	0.0003	0.9888	0.0436
	Genotype*Treatment	0.0044	0.0074	0.0103	0.3789	0.0212
7	Genotype	<0.0001	<0.0001	<0.0001	0.0067	<0.0001
	Treatment	0.0538	0.0001	0.0006	0.0193	0.0197
	Genotype*Treatment	0.0145	0.0183	<0.0001	0.9799	0.0226
10	Genotype	<0.0001	<0.0001	<0.0001	<0.0001	0.0007
	Treatment	0.0026	0.0013	<0.0001	0.0416	<0.0001
	Genotype*Treatment	0.0009	0.0171	<0.0001	0.5281	0.0068

1024

1025

1026

1027

1028

1029

1030 **Figure Legends**

1031

1032 **Figure 1.** Heat map depicting differentially expressed (A) reactive oxygen species [1, cytochrome

1033 p450s; 2, NADPH oxidase; 3, NADH dehydrogenases; 4, amine oxidase and related; 5, copper

1034 methylamine oxidase precursors], (B) nitric oxide [6, nitric oxide synthases; 7, nitrite reductases;

1035 8, NADH-cytochrome b5 reductases], and (C) antioxidant system-associated [9, peroxidases; 10,

1036 catalase; 11, superoxide dismutase] genes between charcoal rot resistant (SC599) and susceptible

1037 (Tx7000) sorghum genotypes in response to *Macrophomina phaseolina* inoculation at 7 days post-

1038 inoculation. Red, green, and black colors represent up-regulated, down-regulated, and non-

1039 differentially expressed genes, respectively, after pathogen inoculation compared to mock-

1040 inoculated control treatment with sterile phosphate-buffered saline. See Supplementary Table 1

1041 for a detailed list of genes, differential expression levels, and q-values.

1042

1043 **Figure 2.** Comparison of the mean total free radical content (sum of the reactive oxygen and

1044 nitrogen species as measured by dichlorodihydrofluorescein (DCF) concentration) among two

1045 treatments (CON, MP) in charcoal rot susceptible (BTx3042, Tx7000) and resistant (SC599,

1046 SC35) genotypes at 4, 7, and 10 days post-inoculation (DPI). Treatment means followed by

1047 different letters within each genotype at a given DPI are significantly different. Treatment means

1048 with "ns" designations are not significantly different within each genotype at a given DPI at $\alpha =$

1049 0.05. Error bars represent standard errors. CON = phosphate-buffered saline mock-inoculated

1050 control, MP = *Macrophomina phaseolina*-inoculated.

1051

1052   **Figure 3.** (A) Detection of nitric oxide (NO) in sorghum stem tissues after staining with 4-amino-

1053   5-methylamino-2',7'-difluorofluorescein diacetate (DAF FM-DA) by confocal microscopy. Cross-

1054   section of a single vascular bundle ("vb") of the charcoal rot susceptible and resistant sorghum

1055   genotypes, Tx7000 and SC599, respectively, after receiving the *Macrophomina phaseolina* (MP;

1056   1st and 3rd rows) and mock-inoculated control (phosphate-buffered saline) treatments (2nd and

1057   4th rows) at 7 days post-inoculation (DPI) (Magnification = 200×). (B) Cross-sections showing

1058   the vascular bundles and surrounding parenchyma (pith) cells of charcoal rot susceptible

1059   (BTx3042, Tx7000) and resistant (SC35, SC599) sorghum genotypes after receiving the *M.*

1060   *phaseolina* and mock-inoculated control treatments at 7 DPI (Magnification = 25×). Stem cross-

1061   sections showing bright green fluorescence correspond to the detection of NO. Lack of bright green

1062   in the "fluorescence" and "overlay" micrographs indicate the absence of NO after both treatments.

1063   Red color corresponds to chlorophyll autofluorescence. pc = parenchyma cells

1064

1065   **Figure 4.** Comparison of the mean peroxidase activity among two treatments (CON, MP) in

1066   charcoal rot susceptible (BTx3042, Tx7000) and resistant (SC599, SC35) genotypes at 4, 7, and

1067   10 days post-inoculation (DPI). Treatment means followed by different letters within each

1068   genotype at a given DPI are significantly different while the treatment means with "ns"

1069   designations within each genotype at a given DPI are not significantly different at $\alpha = 0.05$. Error

1070   bars represent standard errors. CON = phosphate-buffered saline mock-inoculated control, MP =

1071   *Macrophomina phaseolina*-inoculated.

1072

1073   **Figure 5.** Comparison of the mean catalase activity among two treatments (CON, MP) in charcoal

1074   rot susceptible (BTx3042, Tx7000) and resistant (SC599, SC35) genotypes at 4, 7, 10 days post-

1075   inoculation (DPI). Treatment means followed by different letters within each genotype at a given

1076   DPI are significantly different while the treatment means with "ns" designations within each

1077   genotype at a given DPI are not significantly different at α = 0.05. Error bars represent standard

1078   errors. CON = phosphate-buffered saline mock-inoculated control, MP = *Macrophomina*

1079   *phaseolina*-inoculated.

1080

1081   **Figure 6.** Comparison of the mean superoxide dismutase activity (A) among two treatments (CON,

1082   MP) across four sorghum genotypes (BTx3042, Tx7000, SC599, SC35) at 4, 7, and 10 days post-

1083   inoculation (DPI) and (B) among four sorghum genotypes across two treatments at three post-

1084   inoculation stages. Treatment means followed by different letters within a given DPI are

1085   significantly different while the treatment means with "ns" designations are not significantly

1086   different at α = 0.05. Genotype means followed by different letters within a given DPI are

1087   significantly different based on the adjusted *P*-value for multiple comparisons using Tukey-

1088   Kramer's test at α = 0.05 while the genotype means with "ns" designations within a given DPI are

1089   not significantly different. Error bars represent standard errors. CON = phosphate-buffered saline

1090   mock-inoculated control, MP = *Macrophomina phaseolina*-inoculated.

1091

1092   **Figure 7.** Comparison of the mean malondialdehyde content among two treatments (CON, MP)

1093   in charcoal rot-susceptible (BTx3042, Tx7000) and -resistant (SC599, SC35) genotypes at 4, 7,

1094   and 10 days post-inoculation (DPI). Treatment means followed by different letters within each

1095   genotype at a given DPI are significantly different. Treatments with "ns" designations are not

1096   significantly different within each genotype at a given DPI at α = 0.05. Error bars represent

1097   standard errors. CON = phosphate-buffered saline mock-inoculated control, MP = *Macrophomina*

1098   *phaseolina*-inoculated.

1099

1100

1101

1102

1103

1104

1105

1106

1107

1108

1109

1110
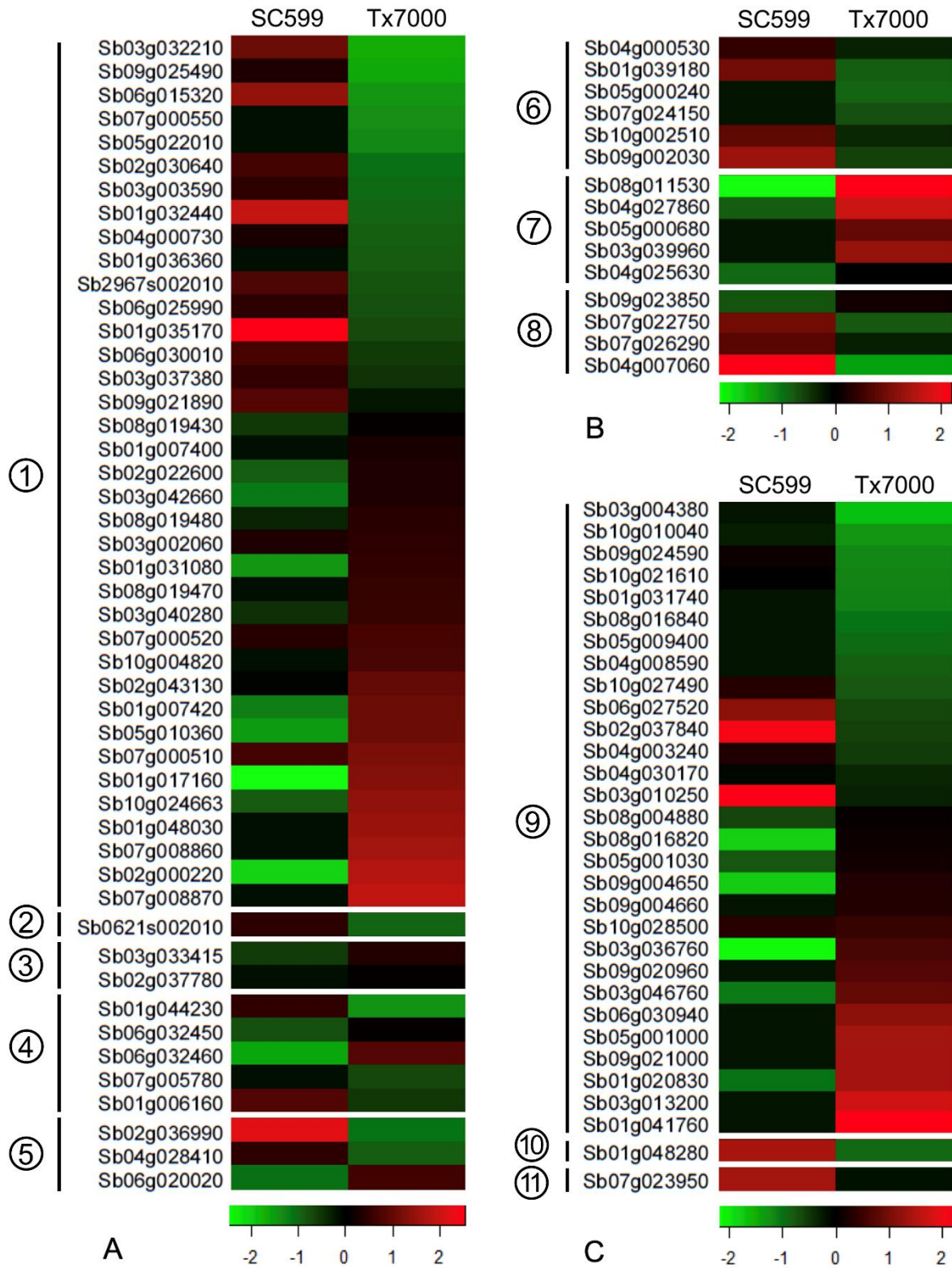
1111

1112

1113

1114
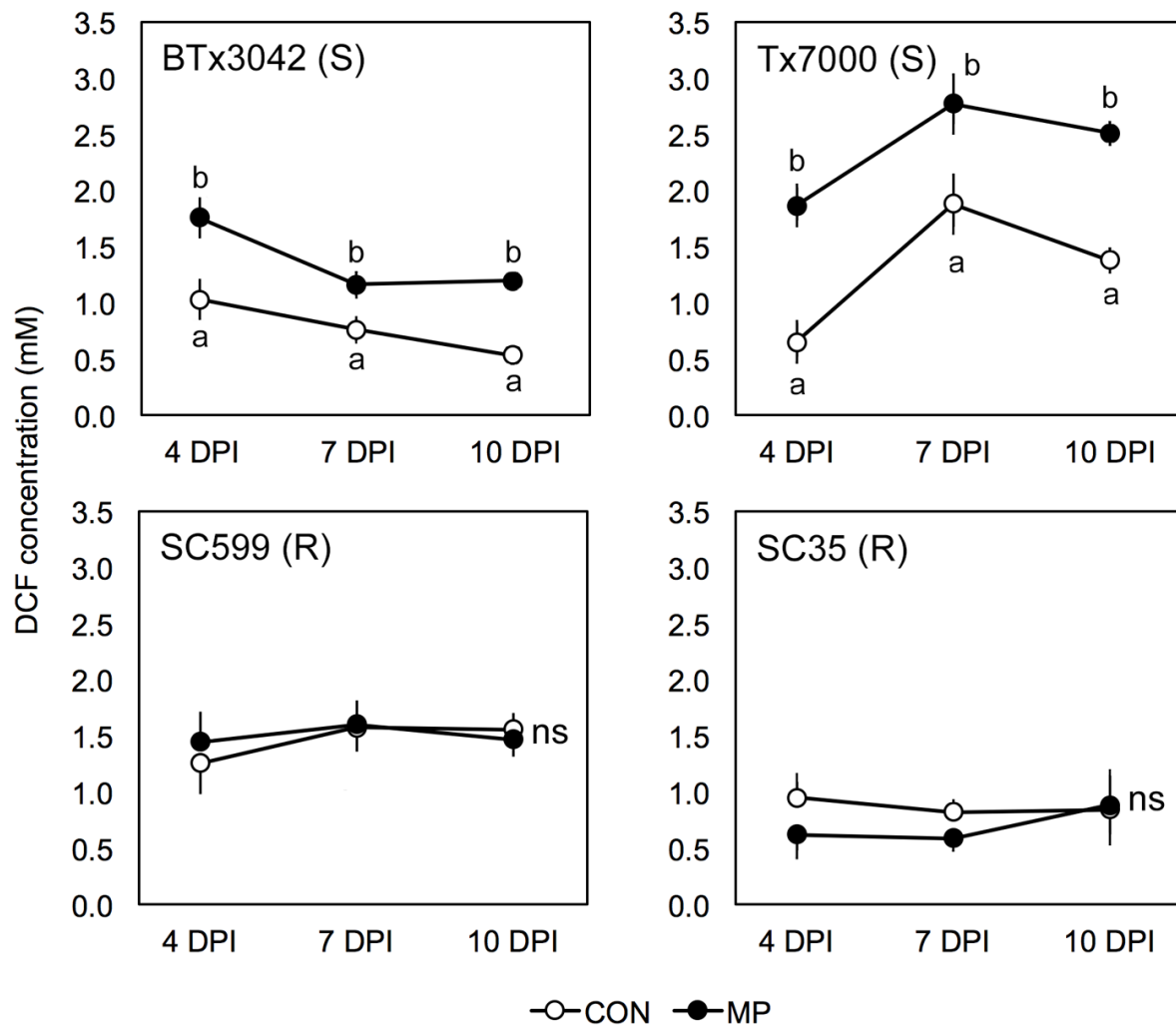
1115

1116

1117

1118

1119

1120   **Figure 1.**
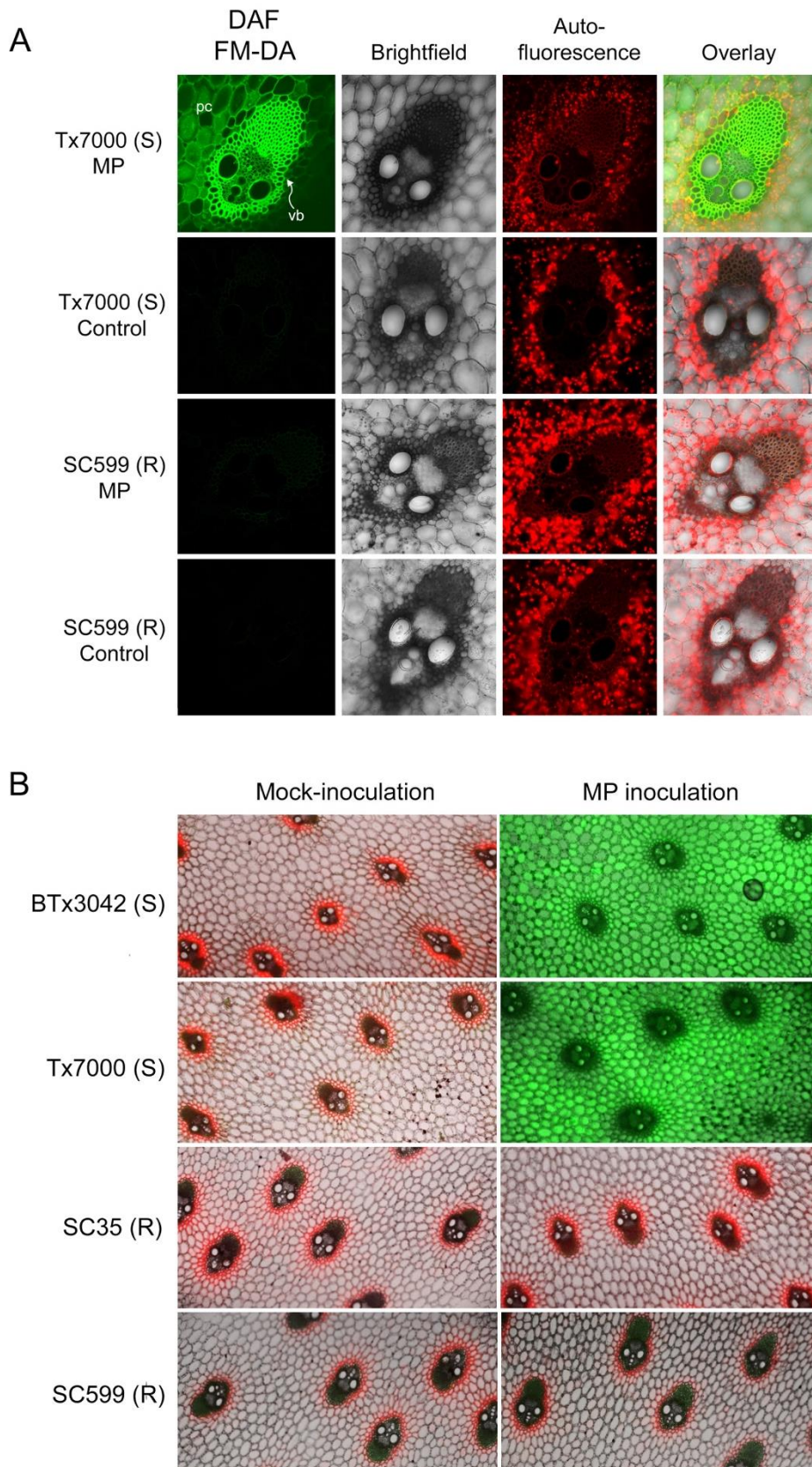
1121 **Figure 2.**

1122

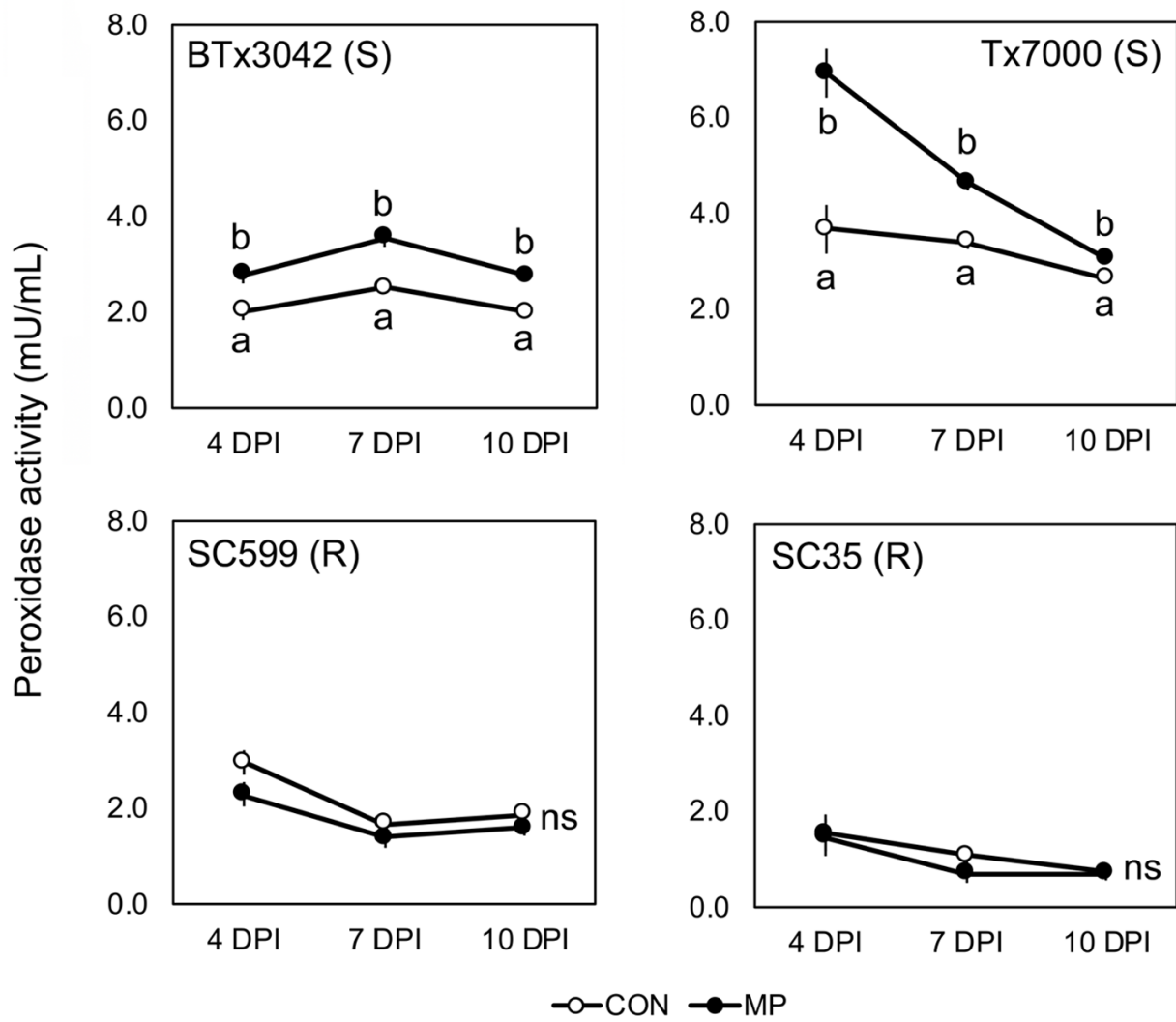1123

1124

1125

1126

1127

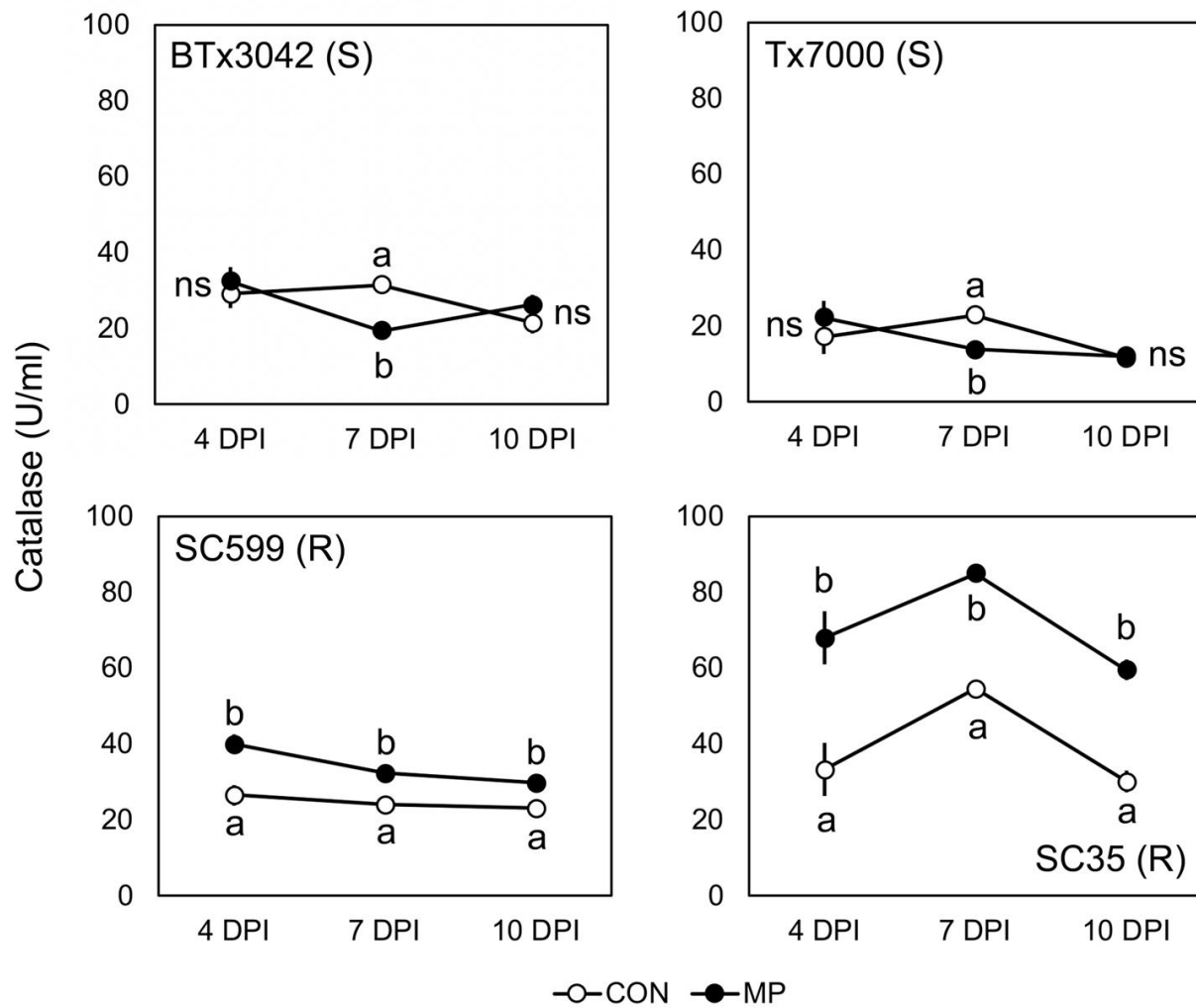1128

1129

1130 **Figure 3.**
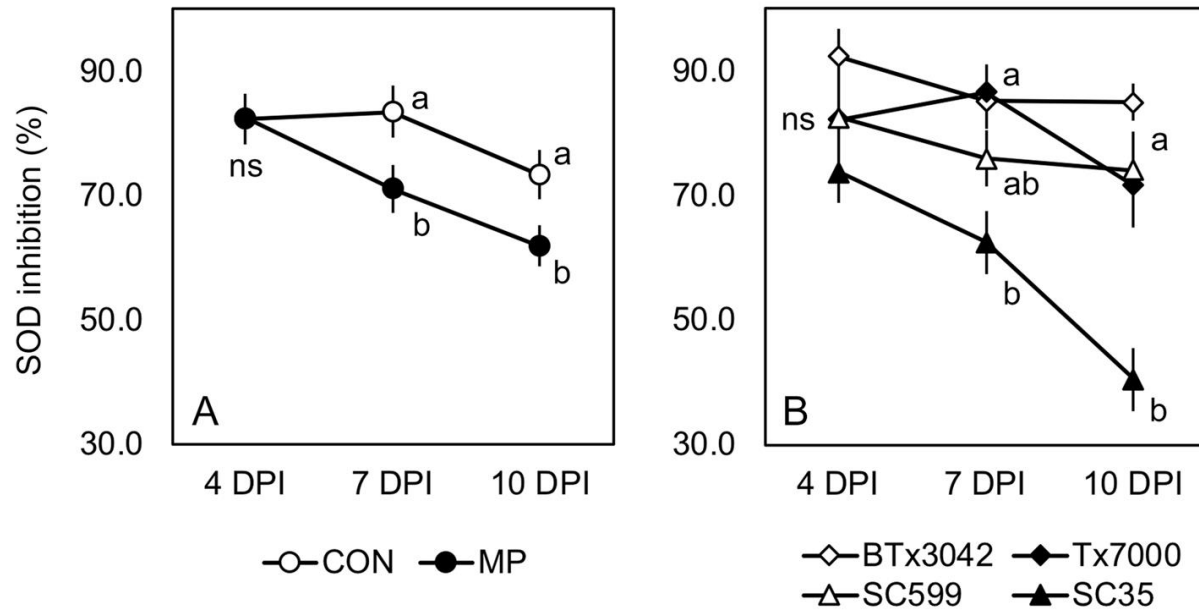
1132   **Figure 4.**

1133
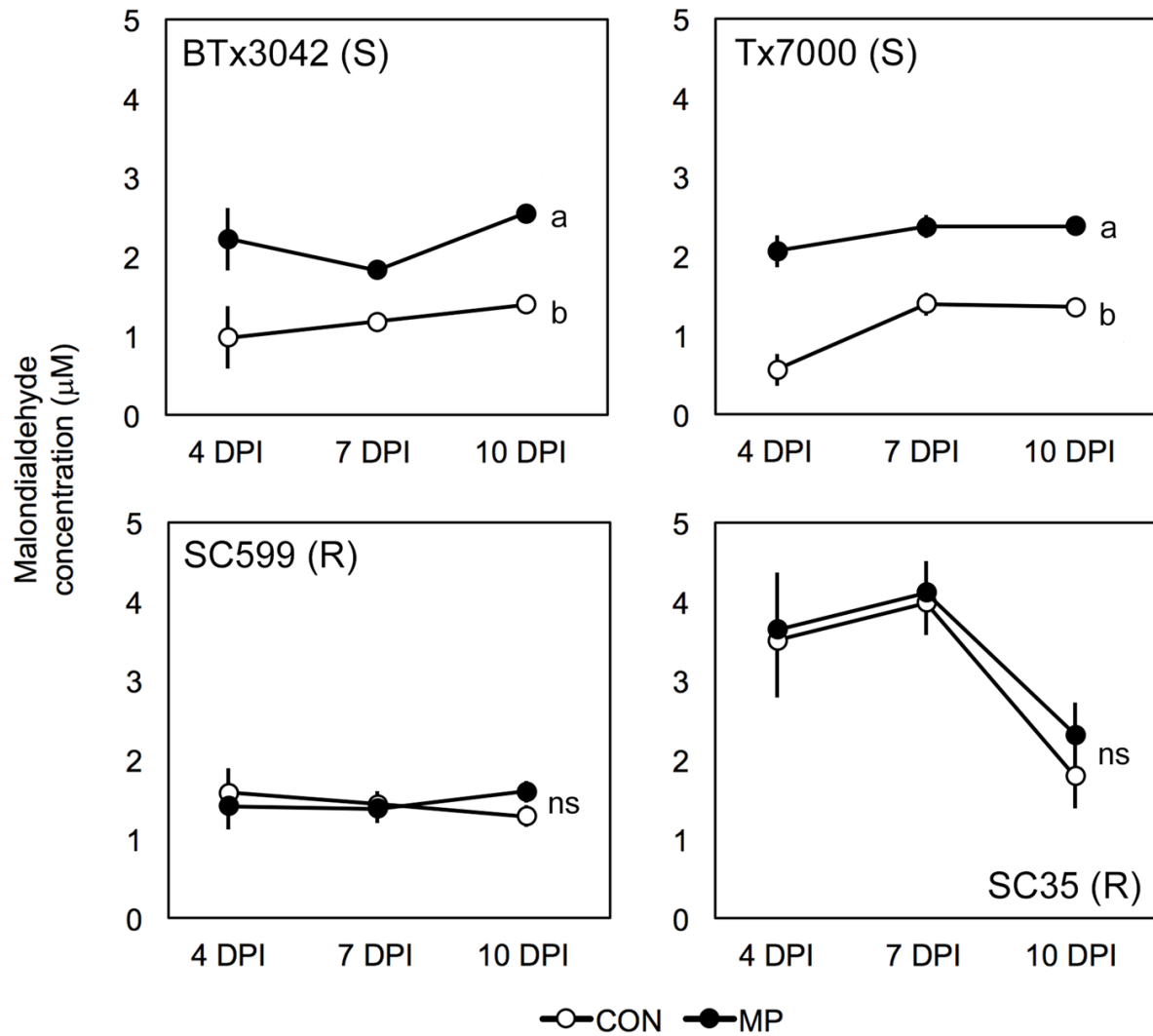
1134

1135 **Figure 5.**

1136

1137   **Figure 6.**

1138

1139   **Figure 7.**

1140

Supplementary Table 1. Significantly (q < 0.05) differentially expressed genes related to host oxidative stress and antioxidant system between SC599 (charcoal rot resistant) and Tx7000 (charcoal rot susceptible) sorghum genotypes in response to *Macrophomina phaseolina* inoculation at 7 days post inoculation.

Gene annotation	Metabolic pathway	Gene ID	Geno × Trt* q-value	SC599 (MP-CON)†		Tx7000 (MP-CON)	
				log2 DE‡	q-value	log2 DE	q-value
Cytochrome P450	Unknown	*Sb03g032210*	9.3E-12	1.29	0.1893	-6.03	5.4E-06
		Sb09g025490	4.1E-03	0.48	0.9194	-5.87	1.2E-06
		Sb06g015320	1.7E-04	1.70	0.2952	-5.17	3.0E-04
		Sb07g000550	7.1E-03	-	-	-4.82	1.6E-04
		Sb05g022010	3.8E-03	-	-	-4.58	2.6E-03
		Sb02g030640	2.1E-02	0.88	0.7566	-3.63	3.2E-02
		Sb03g003590	1.1E-03	0.65	0.7830	-3.42	9.5E-05
		Sb01g032440	5.6E-04	2.22	0.0601	-3.18	6.8E-02
		Sb04g000730	1.4E-04	0.42	0.8226	-2.91	7.9E-04
		Sb01g036360	2.1E-04	0.00	0.9992	-2.79	5.4E-10
		Sb2967s002010	9.2E-04	0.97	0.4544	-2.58	4.3E-05
		Sb06g025990	3.4E-06	0.64	0.3355	-2.39	3.6E-07
		Sb01g035170	1.8E-09	2.84	0.0001	-2.08	6.9E-09
		Sb06g030010	2.7E-06	0.91	0.1931	-1.58	1.8E-04
		Sb03g037380	1.9E-03	0.69	0.5468	-1.21	4.4E-05
		Sb09g021890	4.9E-02	1.06	0.2254	-0.22	5.9E-01
		Sb08g019430	3.0E-02	-0.44	0.8043	1.01	1.7E-02
		Sb01g007400	1.1E-02	-	-	1.74	4.6E-03
		Sb02g022600	2.1E-03	-0.80	0.5789	1.94	1.7E-04
		Sb03g042660	2.5E-05	-1.10	0.4289	1.98	4.2E-07
		Sb08g019480	1.1E-02	-0.22	0.9559	2.34	8.3E-05
		Sb03g002060	1.9E-02	0.49	0.7760	2.41	2.1E-07
		Sb01g031080	2.8E-05	-1.41	0.2741	2.65	2.8E-09
		Sb08g019470	4.6E-02	-	-	2.83	1.7E-02
		Sb03g040280	1.2E-02	-0.35	0.9368	2.94	7.9E-06
		Sb07g000520	3.4E-04	0.57	0.7335	3.53	3.9E-16
		Sb10g004820	3.8E-03	-	-	3.65	6.4E-05
		Sb02g043130	1.6E-04	0.12	0.9833	4.74	5.2E-15
		Sb01g007420	7.1E-09	-1.16	0.2596	4.96	5.6E-15
		Sb05g010360	7.6E-10	-1.45	0.2546	5.00	1.7E-30
		Sb07g000510	1.1E-04	0.89	0.3230	5.46	2.2E-06
		Sb01g017160	6.1E-20	-2.51	0.0011	5.90	1.1E-32

		Sb10g024663	5.8E-16	-0.79	0.4097	6.43	5.0E-10
		Sb01g048030	4.9E-02	-	-	6.75	8.3E-08
		Sb07g008860	2.2E-05	-	-	7.15	2.2E-09
		Sb02g000220	2.1E-06	-2.03	0.1498	7.87	2.9E-64
		Sb07g008870	1.3E-03	-	-	8.27	2.2E-12
NADPH oxidase	Apoplastic superoxide generation	*Sb0621s002010*	6.4E-05	0.61	0.7974	-3.20	8.4E-29
NADH dehydrogenase 1 alpha subcomplex, assembly factor 1	Respiratory chain Complex I	*Sb03g033415*	1.1E-04	-0.47	0.7917	2.14	3.6E-05
NADH dehydrogenase iron-sulfur protein 4, mitochondrial precursor		*Sb02g037780*	9.4E-03	-0.01	0.9979	0.97	1.8E-05
Amine oxidase, flavin-containing, domain containing protein,	Unknown	*Sb01g044230*	1.4E-02	0.68	0.8358	-4.96	1.8E-03
		Sb06g032450	3.3E-03	-0.68	0.4749	0.92	1.2E-03
		Sb06g032460	1.3E-15	-1.58	0.0617	4.10	1.5E-58
		Sb07g005780	8.0E-04	-	-	-2.04	1.3E-03
Amine oxidase-related		*Sb01g006160*	1.1E-03	1.04	0.2741	-1.39	2.9E-03
Copper methylamine oxidase precursor		*Sb02g036990*	9.3E-12	2.52	0.0001	-3.71	1.1E-03
		Sb04g028410	2.8E-06	0.61	0.6758	-2.84	1.4E-12
		Sb06g020020	1.7E-20	-1.02	0.1013	3.33	6.1E-48
EC 1.14.13.39, Nitric oxide synthase (NOS)	Citrulline-nitric oxide cycle	*Sb04g000530*	1.4E-02	0.42	0.7458	-0.82	1.1E-02
		Sb01g039180	1.0E-03	0.78	0.7386	-2.84	6.5E-04
		Sb05g000240	1.1E-02	-	-	-3.11	7.4E-02
		Sb07g024150	4.2E-02	-	-	-2.41	1.3E-01
		Sb10g002510	1.7E-04	0.67	0.3981	-1.01	1.4E-04
		Sb09g002030	3.7E-02	1.02	0.6437	-1.87	1.4E-02
EC 1.7.2.1, Nitrite reductase (NO-forming)	Nitrate reduction I	*Sb08g011530*	2.1E-11	-1.37	0.4544	9.34	2.9E-76
		Sb04g027860	1.3E-02	-0.42	0.9108	7.48	2.1E-31
		Sb05g000680	3.0E-03	-	-	4.00	7.0E-05
		Sb03g039960	7.7E-05	-	-	5.66	1.0E-11
		Sb04g025630	4.3E-02	-0.49	0.4999	0.27	2.9E-01
EC 1.7.1.1, NADH-cytochrome b5 reductase	Nitrate reduction II (assimilatory)	*Sb09g023850*	2.4E-03	-0.38	0.7270	1.04	7.2E-04
		Sb07g022750	2.9E-05	0.80	0.6184	-2.71	3.6E-27
		Sb07g026290	1.1E-02	0.64	0.4211	-0.75	4.2E-02
		Sb04g007060	1.4E-06	1.58	0.3029	-5.19	5.1E-18
Peroxidase activity	H_2O_2 detoxification	*Sb03g004380*	1.1E-03	-	-	-6.32	3.9E-27
		Sb10g010040	2.2E-02	-0.06	0.9950	-4.85	9.3E-04
		Sb09g024590	2.0E-06	0.22	0.9588	-4.31	2.2E-08
		Sb10g021610	4.0E-05	0.10	0.9837	-4.14	6.1E-16
		Sb01g031740	2.2E-02	-	-	-4.08	1.0E-02
		Sb08g016840	3.3E-03	-	-	-3.58	3.3E-05

		Sb05g009400	1.7E-02	-	-	-3.33	5.4E-02
		Sb04g008590	2.7E-02	-	-	-2.89	1.0E-01
		Sb10g027490	3.5E-02	0.34	0.9445	-2.66	2.8E-03
		Sb06g027520	5.0E-04	0.93	0.2159	-2.08	1.3E-03
		Sb06g027520	5.0E-04	0.93	0.2159	-2.08	1.3E-03
		Sb02g037840	4.9E-03	1.55	0.2380	-1.96	8.4E-02
		Sb04g003240	3.3E-02	0.31	0.9327	-1.70	1.1E-07
		Sb04g030170	1.9E-03	0.07	0.9719	-0.97	1.4E-03
		Sb03g010250	7.6E-03	1.58	0.1351	-0.80	2.9E-01
		Sb08g004880	3.0E-02	-0.28	0.8646	0.73	1.7E-02
		Sb08g016820	8.7E-03	-1.08	0.2781	1.01	2.6E-02
		Sb05g001030	3.4E-02	-0.39	0.8267	1.08	2.2E-02
		Sb09g004650	3.3E-03	-1.06	0.4214	1.57	9.0E-05
		Sb09g004660	3.5E-02	-	-	1.72	3.1E-01
		Sb10g028500	4.8E-02	0.36	0.9018	2.29	3.2E-07
		Sb03g036760	1.8E-07	-1.33	0.1929	2.92	2.8E-05
		Sb09g020960	3.8E-02	-	-	3.35	2.2E-02
		Sb03g046760	1.4E-06	-0.60	0.8320	3.94	1.5E-64
		Sb06g030940	1.2E-04	-	-	5.27	1.9E-04
		Sb05g001000	2.6E-10	-	-	6.07	1.4E-08
		Sb09g021000	5.3E-04	-	-	6.13	4.5E-06
		Sb01g020830	2.9E-08	-0.56	0.8097	6.17	1.1E-21
		Sb03g013200	4.2E-04	-	-	7.65	1.0E-10
		Sb01g041760	3.4E-04	-	-	9.28	8.2E-27
Catalase	H_2O_2 detoxification	Sb01g048280	1.5E-04	1.10	0.3804	-3.23	1.2E-06
Superoxide dismutase	Superoxide dismutation	Sb07g023950	2.1E-02	1.07	0.1760	-0.27	4.4E-01

*Geno × Trt = genotype by treatment interaction where treatment consists of *M. phaseolina* and control inoculations. †MP = *M. phaseolina*, CON =control. ‡ log2 DE = log2 fold differential expression.